International Journal of Fatigue 189 (2024) 108550

Contents lists available at ScienceDirect

International Journal of Fatigue

journal homepage: www.elsevier.com/locate/ijfatigue

Dynamic characteristics of compacted landfill waste material from cyclic triaxial tests

Sangharsha Bhandari [a], Behzad Fatahi [a,*], Waranga Habaraduwa Peellage [a], Hadi Khabbaz [a], Haleh Rasekh [a], Jeff Hsi [b]

[a] School of Civil and Environmental Engineering, University of Technology Sydney (UTS), Sydney, Australia
[b] EIC Activities Pty Ltd (a Member of the CIMIC Group), Sydney, Australia

ARTICLE INFO

Keywords:
Cyclic triaxial test
Reconstituted landfill waste
Cyclic properties
Resilient Modulus
Damping ratio

ABSTRACT

This study conducted a series of cyclic and monotonic triaxial tests on reconstituted landfill waste material from a closed landfill site in Sydney, Australia, to assess its dynamic behaviour under various testing conditions. Specifically, the effects of cyclic deviatoric stress, loading frequency, and effective confining stress on the cumulative plastic axial strain, resilient modulus, and damping ratio under undrained cyclic loading conditions were investigated. Results indicated that the plastic deformation, resilient modulus, and material damping are significantly influenced by dynamic stress and confining stress, with a lesser impact from loading frequency. Notably, as the number of loading cycles increased, the cumulative plastic axial strain and resilient modulus exhibited an increase, whereas the damping ratio decreased. Furthermore, increasing cyclic deviatoric stress led to an increase in both cumulative plastic axial strain and damping ratio, while an increase in confining stress resulted in a decrease in these parameters. Conversely, the resilient modulus showed an increase with rising cyclic deviatoric stress and confining stress. The influence of loading frequency on cumulative plastic axial strain and resilient modulus was minor, and its effect on the damping ratio was rather negligible. The study observed that initial loading cycles caused rearrangement and reorientation of waste components and the mobilisation of fibres with tensile forces as loading progressed, suggesting that these landfill waste samples behaved comparably to fibrous soil with randomly distributed fibres. Through nonlinear regression analysis, an empirical relationship for cumulative plastic axial strain incorporating cyclic deviatoric stress, confining stress, number of cycles, and frequency was derived. This research contributes valuable insights into the behaviour of compacted landfills as railway subgrades, providing a foundation for informed decision-making in the design of transport infrastructure over closed landfill sites.

1. Introduction

As a part of many infrastructure development initiatives, landfill sites, formerly located at a considerable distance away from urban centres, are now closer to or within urban areas, and authorities cannot bypass them efficiently and thus are planning their strategic reuse. Indeed, there are over 2800 landfill sites in Australia, including both regulated and unregulated ones [1], and numerous transport infrastructure projects are now under review or construction, such as WestConnex St Peters Interchange and Moorebank Intermodal Terminal in Sydney, which are partially positioned on closed landfills.

Construction of transport infrastructure over the closed landfills presents various environmental and engineering challenges, including structural stability, short-term and long-term settlement problems, contamination of the surrounding environment and generation of toxic gases. Environmental problems associated with waste and its incineration, remediation techniques and various waste management approaches have been of interest to several researchers [2–6]. The heterogeneous and often unpredictable characteristics of the materials discarded in landfills are the fundamental reasons behind the engineering challenges. This heterogeneity creates uncertainty in the response of the waste material under traffic/train loads in transport infrastructure. Extensive research studies have been undertaken to explore the properties of landfill waste, such as unit weight, moisture

* Corresponding author at: School of Civil and Environmental Engineering, University of Technology, Sydney (UTS), City Campus PO Box 123 Broadway NSW 2007, Australia.
E-mail address: Behzad.Fatahi@uts.edu.au (B. Fatahi).

https://doi.org/10.1016/j.ijfatigue.2024.108550
Received 13 May 2024; Received in revised form 11 July 2024; Accepted 11 August 2024
Available online 12 August 2024

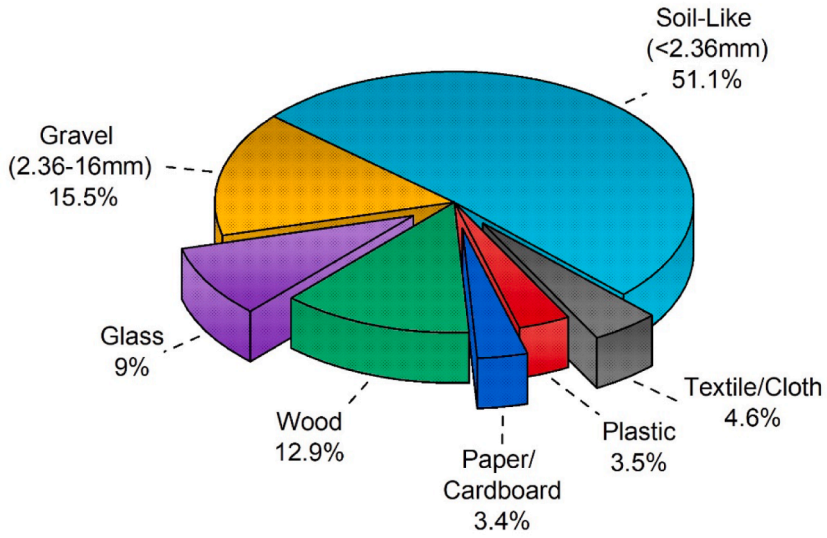

(a)

(b)

Fig. 1. (a) Composition of the landfill waste retrieved from a landfill site in Sydney, and (b) images of waste sample mix and various components.

content, permeability, waste composition, and shear strength, in the past few decades [7–20]. These geotechnical parameters are expected to mitigate engineering design challenges, ensuring the sustainability and resiliency of structures exposed under static loading. However, the behaviour of the substructure of the railway track, such as the railway subgrade, under traffic loads is governed by both static and dynamic responses. In evaluating the potential integration of closed landfills into railway expansion plans, it is imperative for railway engineers to better understand both the static and cyclic response of landfill waste.

Numerous researchers have conducted investigations to evaluate the performance of railway subgrade under repeated loading conditions [21–25]. For example, a series of cyclic triaxial tests were conducted to understand the cyclic behaviour of soft soil under diverse loading scenarios, number of cycles, loading frequency and confining stress

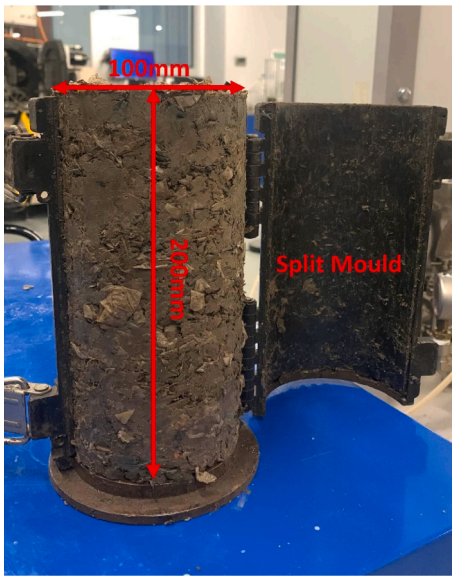

(a)

(b)

Fig. 2. (a) Compacted landfill waste sample ready for cyclic triaxial test, and (b) sample sealed with rubber membrane.

conditions, and the findings revealed that these parameters have a notable impact on the response of the soil [26,27]. Various existing literature has presented that the dynamic stress level and loading frequency on the soil vary with train speed, impacting the accumulation of the permanent deformation and the subgrade resilient modulus [28]. Furthermore, intensive research was also carried out to assess the cyclic response of recycled waste materials such as recycled rubber and plastic products, demolition waste and recycled glass in railway substructures, enhancing the sustainability and resilience of the railway infrastructure, proposing their addition into the railway substructure [29,30]. It can be noted that the impacts of parameters like cyclic deviatoric stress, loading frequency, and confining stress are substantial in determining the behaviour of the subgrade material under cyclic loads on railway tracks.

While numerous studies have been carried out to understand the dynamic response of various soil types and recycled waste materials, there are limited research conducted to understand the behaviour of landfill waste as the railway subgrade. However, various research studies have been undertaken regarding the dynamic properties of landfill materials relevant to the seismic analysis, focusing on wave propagation characteristics of the material. Indeed, seismic parameters like shear wave velocity (V_s), maximum shear modulus (G_{max}), and the damping ratio associated with energy dissipation have been areas of interest for researchers over the past few decades [10,15,31–34]. Indeed, the waste composition and confining stress affect the maximum shear modulus and the damping ratio. These effects are due to the presence of fibrous waste, indicating the importance of the reinforcement effect [35]. Likewise, consistent results presented across diverse literature sources indicate a higher dynamic shear modulus value with a progressive rise in confining stress [36]. Similarly, several researchers agreed that the damping ratio shows marginal to notable variation with increasing confining stress of municipal solid waste [33,37,38]. Studies performed at a lower frequency range suggested that loading frequency has a very modest influence on the shear modulus and damping ratio of municipal solid waste [15].

Reiterating the fact that most of the past research studies on landfill waste primarily focused on dynamic characteristics for seismic analysis, there is a great urgency to understand the response of the landfill waste under cyclic load scenarios replicating the closed landfill sites as a railway subgrade. This research aims to fill this gap by providing comprehensive insight into cyclic loading response through laboratory investigation. Eighteen cyclic triaxial tests have been conducted to understand the impact of cyclic deviatoric stress, loading frequency and confining stress on cumulative plastic deformation, resilient modulus and damping ratio of the landfill waste materials retrieved from a landfill site in Sydney. This study seeks to foster an understanding of the dynamic response of landfills, addressing the requirements of railway designers and providing a reliable reference to make informed decisions when designing and building railway track over closed landfill sites.

2. Laboratory experimental investigation

The laboratory investigation in this study primarily comprised of analysing the waste composition from samples collected from a landfill site in airtight barrels, preparing the reconstituted samples, and testing the sample under cyclic triaxial loading in saturated conditions. The following section provides a detailed explanation of sample preparation and laboratory investigation.

2.1. Sample preparation

The material for the laboratory investigation was obtained from a closed landfill site in Sydney, NSW, Australia, which had been in operation for 19 years before its closure. Waste material was collected from a 3 m deep test pit and stored in airtight barrels to retain the field moisture and then transferred to the geotechnology laboratory of the University of Technology Sydney for testing. An initial visual screening of the waste revealed the primary components as textile/cloth, paper/cardboard, wood, plastic, glass, gravel, and soil-like components.

The adopted methodology of characterising waste material is comparable to the approach recommended by Zekkos [15] and Bray et al. [7]. The landfill waste from the barrel was segregated using a 16 mm sieve to determine the waste composition. The sieve size was chosen to ensure that the maximum particle size remained at one-sixth of the sample diameter of 100 mm to be used in the cyclic triaxial test. This segregation was beneficial as the material smaller than 16 mm was predominantly composed of soil, gravel, and some fraction of the waste components such as wood, glass and plastics. Conversely, the materials retained on the 16 mm sieve were largely composed of waste components and gravels larger than 16 mm. The fraction of material passed through the 16 mm sieve underwent further classification into soil-like (less than 2.36 mm) and gravel (between 2.36 and 16 mm). Gravel exceeding 16 mm in size was then mechanically reduced in size. For this

classification, the material passed through the 16 mm sieve was sieved again through a 2.36 mm sieve after oven-drying.

Furthermore, the coarse fraction was segregated into textile/cloth, plastic, paper/ cardboard, wood and glass and separated into two categories: (a) stiff materials like wood and glass and (b) fibrous materials like textile/cloth, plastic, and paper/ cardboard. Stiff materials were further reduced in size, ensuring that they pass through the 16 mm sieve. However, fibrous materials such as cloth, plastic and paper were shredded up to a maximum particle size of 25 mm, considering their tendency to fold during the sample preparation. In addition to this, a minor portion of the waste, which included items such as small metal pieces that could not be further reduced in size, was excluded from the sample. This exclusion was necessary as these components do not precisely represent the overall volume of the waste, and the high unit weight of such materials can occasionally lead to an inconsistent weight percentage. Excluding these items ensured a more representative sample

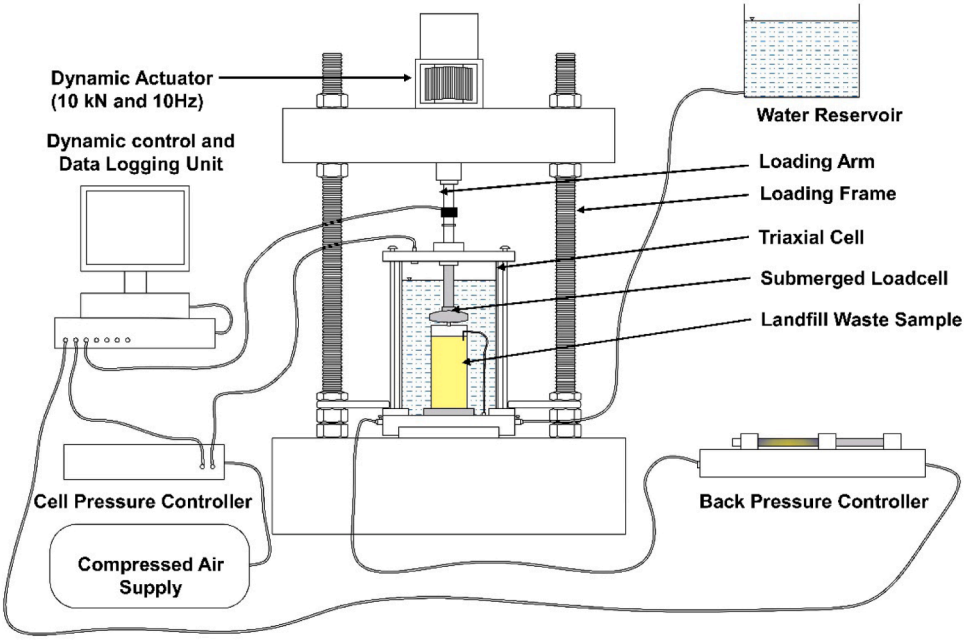

(a)

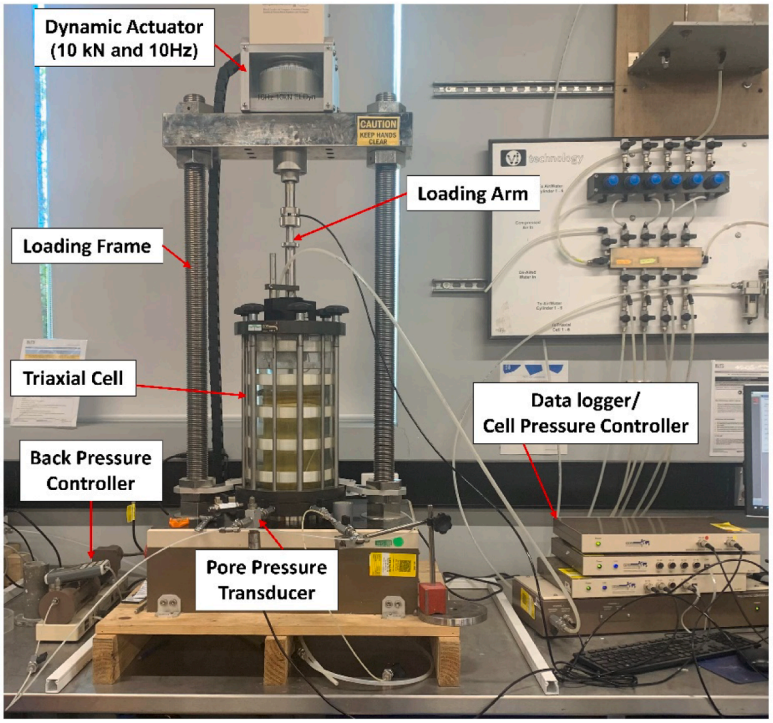

(b)

Fig. 3. (a) Schematic diagram of the cyclic triaxial setup, and (b) GDS cyclic triaxial setup capacity (10kN and 10 Hz) used in this study (c) Three-dimensional loading scheme adopted in this study.

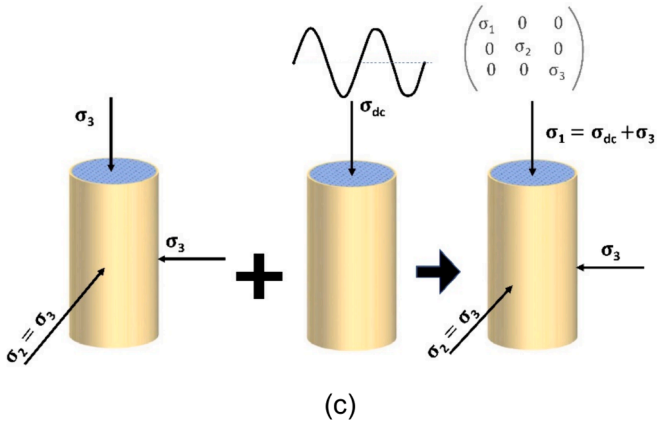

Fig. 3. (*continued*).

Table 1
Summary of the monotonic and cyclic triaxial tests performed on compacted landfill waste material in this study.

Test No.	Loading Frequency, *f* (Hz)	Confining stress, σ'_3 (kPa)	Cyclic Deviatoric Stress, σ_{dc} (kPa)	Number of Cycles, *N*
M1	Monotonic	20	–	–
M2	Monotonic	40	–	–
M3	Monotonic	80	–	–
M4	Monotonic	120	–	–
S1	1	20	20	50,000
S2	1	20	40	50,000
S3	1	20	60	50,000
S4	1	20	80	50,000
S5	1	20	100	50,000
S6	2	20	20	50,000
S7	2	20	40	50,000
S8	2	20	60	50,000
S9	2	20	80	50,000
S10	2	20	100	50,000
S11	5	20	20	50,000
S12	5	20	40	50,000
S13	5	20	60	50,000
S14	5	20	80	50,000
S15	5	20	100	50,000
S16	2	40	40	50,000
S17	2	80	40	50,000
S18	2	120	40	50,000

suitable for testing, as also recommended by Zekkos [15]. The composition of the waste material adopted in this study is presented in Fig. 1a.

Representative specimens were collected to assess the organic and overall moisture content, adhering to ASTM D2216 and ASTM D2974 while segregating the waste [39,40]. The organic content of the waste sample ranged from 20 % to 26 %, with an average value of 23 %. The overall moisture content of this collected waste was measured to be 33.6 %. It should be noted that the moisture content of the different waste components was measured as textile/cloth: 36 %, paper: 125 %, wood: 111 % and soil-like: 26 %. For measuring the moisture content, the oven drying technique was used, and the oven temperature of 55 °C was maintained to prevent the ignition of organic material [32]. The specific gravity (G_s) was determined for the four representative samples, resulting in measurements of 2.04, 2.13, 2.18, and 2.21, averaging at G_s = 2.14.

For the preparation of the reconstituted sample, soil-like, gravel and waste components were thoroughly mixed, maintaining the composition of the waste and the field moisture condition as shown in Fig. 1b. Deaired distilled water was supplemented to preserve the field moisture content as needed. The unit weight of the reconstituted sample was determined using a standard compaction method referring to ASTM

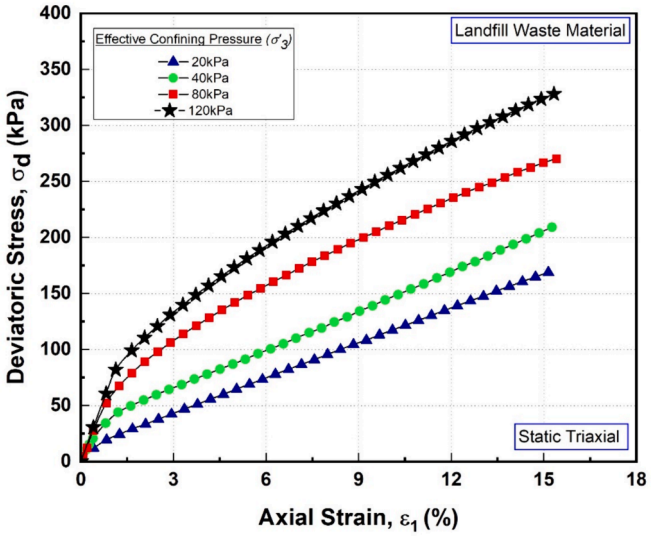

Fig. 4. Result of monotonic triaxial testing conducted in this study.

D698 [41]. The sample's bulk and dry unit weights were measured from the compaction test as 13.96 kN/m^3 and 10.45 kN/m^3, respectively. It should be noted that a total of 22 reconstituted samples were prepared in this study, and all specimens were compacted at the field moisture content of 33.6 %, and subjected to standard compaction energy. For the cyclic triaxial sample preparation, compaction of the specimen within a mould with a height of 200 mm and an internal diameter of 100 mm was carried out in five layers of 40 mm each. The landfill mix prepared for each sample was divided into five equal thicknesses, confirmed by measuring the height continuously, resulting in the total compaction energy of 600 kJ/m^3 corresponding to the standard compaction energy (Fig. 2a). It should be noted that efforts were made to ensure the uniform distribution of the material composition in each compaction layer.

2.2. Laboratory investigation

In this study, four monotonic triaxial tests and eighteen stress-controlled consolidated-undrained dynamic triaxial tests were conducted on the compacted landfill waste material employing the GDS Enterprise Level Dynamic Triaxial Testing System (ELDYN) available in the geotechnology laboratory at the University of Technology Sydney.

As shown in Fig. 3a and Fig. 3b, the adopted ELDYN setup comprised of a triaxial cell supported on a loading frame, cell and back pressure controllers, a pore pressure transducer, a loading ram attached to a

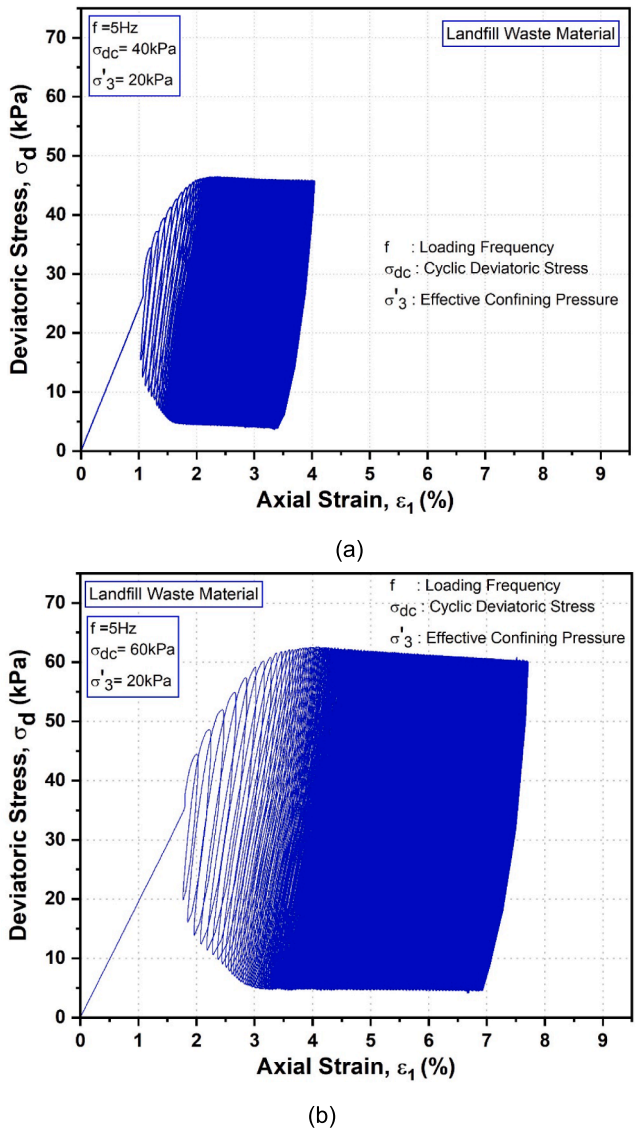

Fig. 5. Cyclic stress–strain curves for compacted landfill waste with loading frequency $(f) = 5$ Hz (a) $\sigma_{dc} = 40$ kPa (b) $\sigma_{dc} = 60$ kPa.

dynamic actuator and a data logger connected to a computer-equipped with GDS software. Cell pressure was applied through the integrated air compressor available at the laboratory, and back pressure was upheld using a GDS enterprise pressure controller. The pore pressure transducer was calibrated and utilised to record the excess pore water pressure throughout the application of the cyclic load. The loading capacity of the load cell and frame was 10 kN with a maximum loading frequency of 10 Hz.

Following the essential checks and calibration of the cyclic triaxial setup, the compacted waste sample was positioned within the triaxial cell, enclosed with a rubber membrane with a thickness of 0.3–0.4 mm, and securely sealed with O-rings (Fig. 2b). The testing stages were saturation and consolidation, followed by cyclic loading. During the saturation stage, de-aired distilled water was supplied into the sample by ramping up the cell pressure and back pressure at a rate of 1 kPa per minute until a back pressure of 300 kPa was reached. A sample was deemed saturated as Skempton's B value of 0.95–0.98 was reached, and the isotropic consolidation phase commenced immediately after. In this study, the saturation stage took approximately 6 to 8 days, while the consolidation stage, which was two-way drained, took approximately 4 to 6 days. Numerous scholars advocated for a low confining pressure range of 15–60 kPa for investigating the behaviour of railway subgrade [28,42,43]. Accordingly, an effective confining stress (σ'_3) of 20 kPa was adopted in this study for the bulk of experiments to simulate the shallow depth conditions typically representing railway subgrade scenarios. In addition, additional effective confining stresses (σ'_3) of 40 kPa, 80 kPa and 120 kPa were selected to study the response of the compacted waste material under various consolidation conditions. The consolidation phase was deemed concluded, once the volume change in the sample became insignificant, monitored via the backpressure/volume controller as the volume of water inflow was less than 1 % over a duration of 30 min.

The fundamental parameters governing the cyclic loading phase are loading frequency, cyclic deviatoric stress, and number of loading cycles. The loading frequency of the moving train depends on train velocity, axle distance and carriage length [44,45]. In general, the stress pulse at the surface of the subgrade attenuates so quickly that the four axles under two adjacent cars generate a single cycle of stress pulse [28]. Thus, a single load cycle represents the adjacent four axles while investigating the dynamic response of the subgrade. Considering this fact and incorporating the wide range of train velocities from 40 km/h to 250 km/h, the loading frequency (f) of 1, 2, and 5 Hz were adopted for this study, which aligns with the loading frequency adopted in numerous other studies for railway infrastructure assessment [28,46,47]. As the train passes through the railway track, cyclic deviatoric stress (σ_{dc}) is induced on the railway subgrade. The dynamic stress amplitude varies based on multiple factors, including axle load, train velocity, track structure, track irregularity, ballast depth, and the type of train [48]. Considering all factors, a wide range of cyclic deviatoric stress (σ_{dc}) 20, 40, 60, 80 and 100 kPa were adopted, covering the expected range from the passenger train to the freight train based on the field measurements reported by Liu et al. [28]. A comparable range of values were embraced by several other researchers working on stress transfer from moving trains to subgrade [26,42,43,49]. The sinusoidal cyclic load was applied to the sample covering 50,000 cycles with a minimum deviatoric stress level of 5 kPa maintained throughout the loading process. The three-dimensional loading scheme and stress tensor for the laboratory testing are schematically presented in Fig. 3c. The adopted cyclic testing scenarios used in this study are summarised in Table 1.

Four monotonic triaxial tests were conducted at four distinct effective confining stresses, namely 20, 40, 80, and 120 kPa, following ASTM D4767. The loading was continued until 15 % strain was attained, with failure being reached if the stress did not peak before reaching this strain threshold. Undrained confined modulus (E_{cu}) calculated for four different confining stresses 20, 40, 80, and 120 kPa were 1.5 MPa, 2.9 MPa, 5.9 MPa, and 7.0 MPa, respectively. Additionally, the failure deviatoric stresses (σ_{df}) at 15 % strain were 167 kPa, 205 kPa, 267 kPa, and 325 kPa for each respective confining stress. Fig. 4 illustrates the results of the monotonic triaxial tests conducted on the compacted landfill waste in this study.

3. Results and discussion

3.1. Cyclic Stress-Strain response

Figs. 5 and 6 present cyclic stress–strain responses of tested landfill waste materials. In particular, Fig. 5 presents the cyclic stress–strain behaviour of reconstituted landfill waste specimens, tested under the loading frequency of 5 Hz, effective confining pressure (σ'_3) of 20 kPa

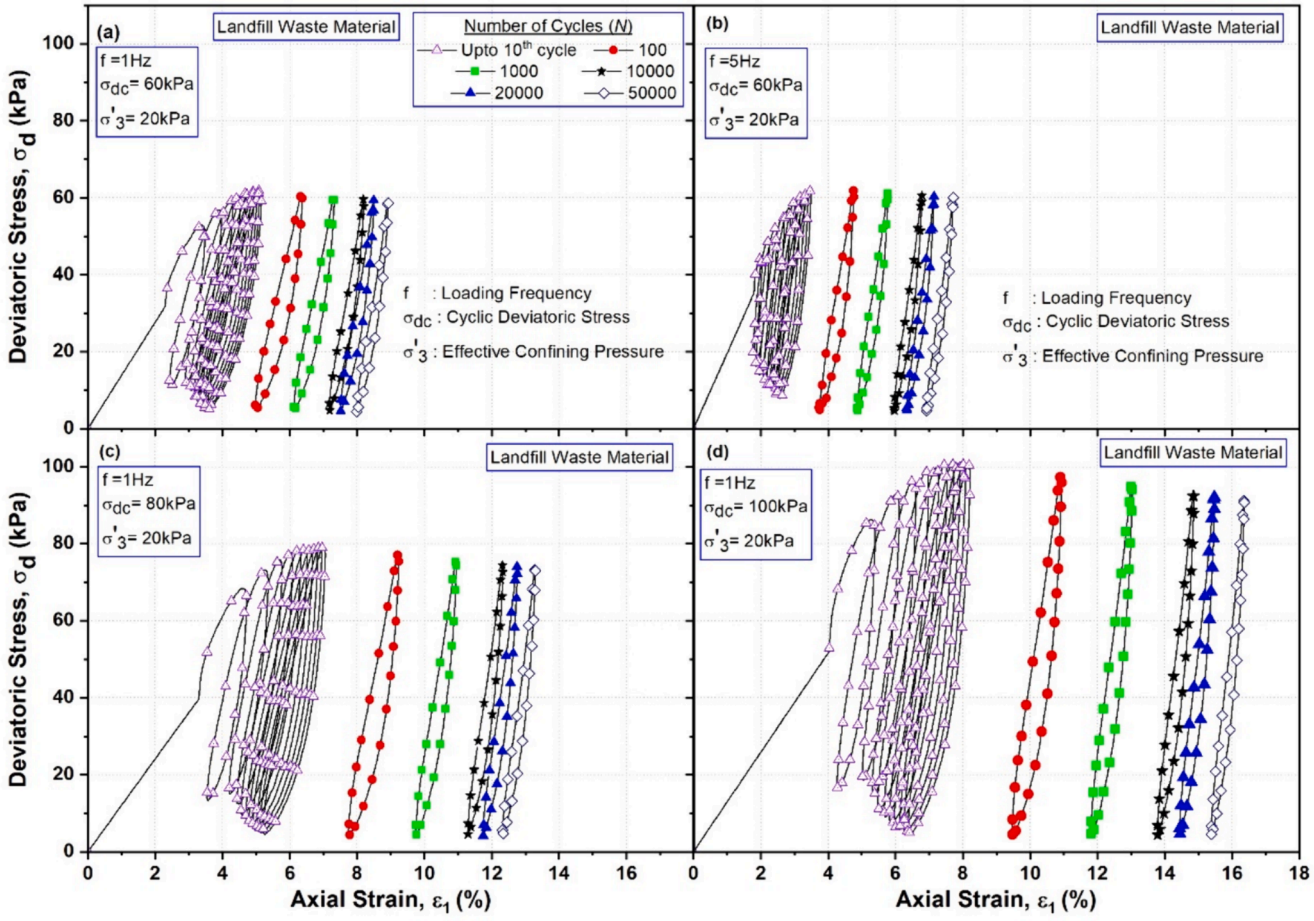

Fig. 6. Hysteresis loops for compacted landfill waste at different number of cycles with (a) $\sigma_{dc} = 60$ kPa and $f = 1$ Hz, (b) $\sigma_{dc} = 60$ kPa and $f = 5$ Hz, (c) $\sigma_{dc} = 80$ kPa and $f = 1$ Hz, (d) $\sigma_{dc} = 100$ kPa and $f = 1$ Hz.

and cyclic deviatoric stresses (σ_{dc}) of 40 kPa and 60 kPa, respectively. It is evident from Fig. 5 that the cyclic stress–strain response of reconstituted landfill waste material is characterised by the formation of hysteresis loops due to distinct loading and unloading paths within a given cycle. Fig. 6 illustrates samples of hysteresis loops of reconstituted landfill waste specimens corresponding to different cycle numbers ranging from 1 to 50000, tested under different loading frequencies and cyclic deviatoric stresses. Referring to Figs. 5 and 6, it is evident that the total axial strain within a hysteresis loop comprises two components: the elastic axial strain and the plastic axial strain. Here, the elastic portion of the axial strain rebounds during the unloading phase, whereas the plastic component remains irrecoverable. Moreover, Figs. 5 and 6 demonstrate the increase in plastic axial strain as the loading cycles progress, albeit at a decreasing accumulation rate. Furthermore, as the cyclic loading progresses across all tested conditions, the hysteresis loops transition from a sparse configuration to a denser arrangement (see Fig. 6), demonstrating cyclic interlocking and fibre mobilisation of the landfill waste material under cyclic loading. Approximately 80–90 % of the strain was observed within the initial 10,000 cycles, with the remaining strain occurring over the subsequent 40,000 cycles.

Moreover, as anticipated, it was observed that the accumulated axial strain at the end of the 50,000 cycle increases with the higher values of cyclic deviatoric stress for a given confining pressure and loading frequency (see Figs. 5, 6a, 6c and 6d). This indicates that the increase in cyclic deviatoric stress notably influences the development of permanent deformation in landfill waste, irrespective of the other testing parameters. Conversely, when maintaining the same cyclic deviatoric stress and confining pressure, an inverse relationship is observed with frequency, as the accumulated axial strain decreases slightly with the increase in loading frequency, as evident in Figs. 5 and 6.

3.2. Cumulative plastic axial strain

As outlined in the previous section (Section 3.1), the irrecoverable component of the axial strain within a given cycle is denoted as the plastic axial strain. Figs. 7 - 9 present the evolution of cumulative plastic axial strain (ε_1^p) in the reconstituted landfill waste samples with loading cycles and for different cyclic deviatoric stresses, confining pressures, and loading frequencies. Moreover, the variation of cumulative plastic axial strain (ε_1^p) corresponding to different cycles during cyclic loading is illustrated in Fig. 10, while Fig. 11 presents the variation of cumulative plastic axial strain at the end of the cyclic loading ($N = 50000$). The cumulative plastic axial strain of the reconstituted landfill waste specimens increases under all tested conditions as the number of cycles progresses, as presented in Figs. 7 - 9. The plastic axial strain accumulates at a significant rate, particularly up to around 10,000 loading cycles, after which its rate gradually diminishes. The rapid increase in the accumulation of plastic axial strain during the initial cycles of loading can be attributed to the rearrangement of the different waste components, such as wood, fibre, glass and gravel within the sample, and the gradual reduction in the strain accumulation rate after certain cycles of loading can be ascribed to the increased interlocking between the

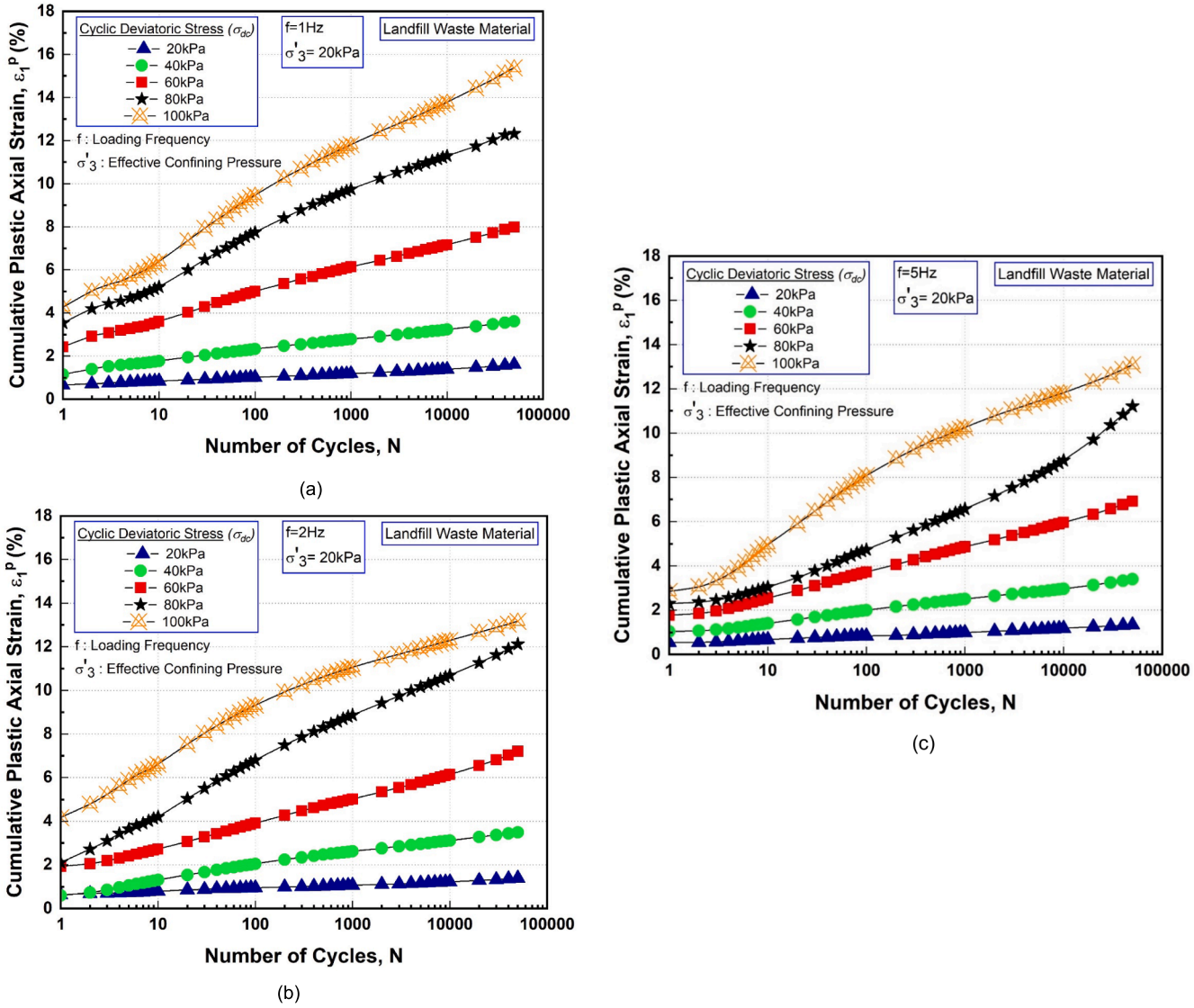

Fig. 7. Results of cumulative plastic axial strain (ε_1^p) vs number of cycles (N) under different cyclic deviatoric stresses (σ_{dc}) (a) $f = 1$ Hz,(b) $f = 2$ Hz,(c) $f = 5$ Hz.

particles as a result of reorientation due to shearing and the mobilisation of the fibres providing reinforcement effect. Fig. 4 illustrates that as the strain increases in monotonic testing, the deviatoric stress does not reach a peak value, indicating the hardening behavior of the material and the reinforcement effect of the fibers at higher strain. In monotonic testing, the stress at 15 % strain is considered the failure stress. In comparison, the sample subjected to 100 kPa cyclic load at a frequency of 1 Hz attained 15.38 % permanent strain after 50,000 cycles. It should be noted that comparable trends were observed by other researchers for fibre-reinforced soils subjected to cyclic loading conditions [50–52].

Furthermore, referring to Figs. 7 and 10a, it is evident that as the cyclic deviatoric stress increases, the cumulative plastic axial strain increases. Moreover, it is noteworthy that the accumulation of plastic strain occurs at a considerably larger rate at higher cyclic deviatoric stress levels (i.e., 80 kPa and 100 kPa) compared to the smaller cyclic deviatoric stress levels (i.e., 20 kPa and 40 kPa). The significant influence of higher cyclic stress on the accumulation of the strain can be attributed to the more pronounced rearrangement of the waste components under higher stress levels. However, as the confining pressure increases, the cumulative plastic axial strain exhibits a significant decline for a given cyclic deviatoric stress and loading frequency, as depicted in Figs. 8 and 10b. For instance, at lower confining pressures of 20 kPa and 40 kPa, the accumulation rate of plastic axial strain is notably higher than that observed at higher confining pressures of 80 kPa and 120 kPa. This behaviour can be explained by the elevated confining stresses imposing increased pressure uniformly on the landfill waste specimen, resulting in enhanced friction between particles, interlocking and waste-fibre matrix interaction as well as reduced void ratio as a result of higher consolidation pressures. Furthermore, as the loading frequency increased, the cumulative plastic axial strain demonstrated a slight decrease, as illustrated in Figs. 9 and 10c. This decline in the cumulative plastic axial strain is particularly noticeable at higher cyclic deviatoric stresses (i.e., 100 kPa) compared to the lower cyclic deviatoric stresses (i.e., 20 kPa). Moreover, Fig. 10c and 11 demonstrate that this reduction is more pronounced in the lower frequency range of 1 Hz to 2 Hz compared to the higher frequency range of 2 Hz to 5 Hz. This behaviour can likely be attributed to time-dependent creep during cyclic loading of the reconstituted landfill waste sample. Higher-frequency cyclic loading results in a shorter reaction time, causing less exposure time to the applied load. However, prolonged exposure at lower frequencies may lead to a greater degree of deformation compared to loading at higher frequencies, which aligns with findings reported in various research studies investigating different types of soil subjected to cyclic loading [53–55].

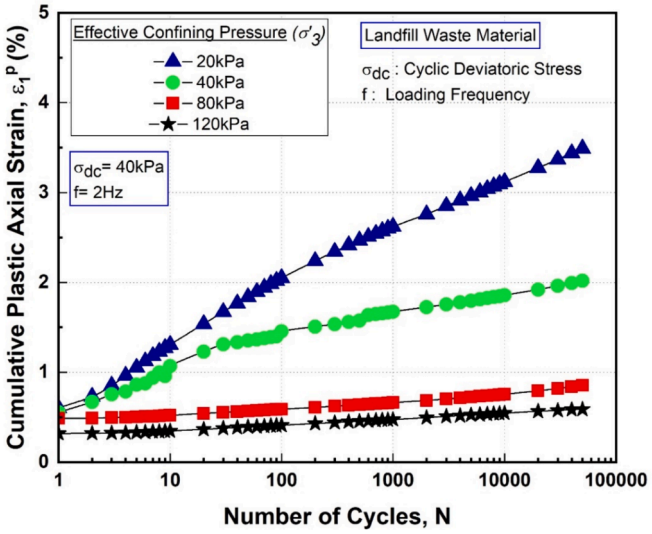

Fig. 8. Results of cumulative plastic axial strain (ε_1^p) vs number of cycles (N) at different effective confining stresses (σ_3') under cyclic deviatoric stress (σ_{dc}) of 40 kPa.

3.3. Prediction of cumulative plastic axial strain

Over the past decades, researchers have formulated numerous empirical and analytical models to predict the cumulative deformation of various geomaterials subjected to cyclic loading conditions. Notably, the power equation that Monismith et al. [56] introduced has emerged as a widely accepted model in predicting the cumulative plastic deformation of various geomaterials. As presented in Figs. 7, 8 and 9, the cumulative plastic axial strain curves of the reconstituted landfill waste specimens exhibited a direct correlation with the cyclic deviatoric stress and the number of cycles, while demonstrating an inverse correlation with loading frequency and confining pressure. Based on all experimental results in this study, an empirical relationship was formulated to predict the plastic axial strain (ε_1^p), as presented in Equation (1).

$$\varepsilon_1^p = \alpha\left(\frac{N}{R_f^{0.5}}\right)^{\beta}\left(\frac{R_q^{0.5}}{tanh(1+1/CSR)}\right)^{\gamma} \tag{1a}$$

$$R_q = \frac{\sigma_{dc}}{\sigma_{df}} \tag{1b}$$

$$R_f = \frac{f}{f_{ref}} \tag{1c}$$

$$CSR = \frac{\sigma_{dc}}{2\sigma'_3} \tag{1d}$$

where, N is the cycle number, CSR is the cyclic stress ratio, R_q is the normalised cyclic deviatoric stress ratio, R_f is the normalised frequency ratio, σ_{dc} is the applied cyclic deviatoric stress, σ'_3 is the effective confining pressure, σ_{df} is the failure deviatoric stress encountered in monotonic triaxial test at 15 % of strain, f is the loading frequency, and f_{ref} is the reference frequency, set as 1 Hz in this study. Moreover, the empirical coefficients α, β and γ were obtained via a data fitting procedure, reflecting the specific attributes of the various constituents in the reconstituted landfill waste specimens. In this study, these coefficients were determined to be $\alpha = 7.8161$, $\beta = 0.1102$, and $\gamma = 2.7038$ through a nonlinear regression process conducted in MATLAB, employing the Nonlinear Least Square method along with the Trust Region Algorithm. The Nonlinear Least Squares method with the Trust Region Algorithm fits models to data by minimising the sum of squared differences between observed and predicted values. The Trust Region

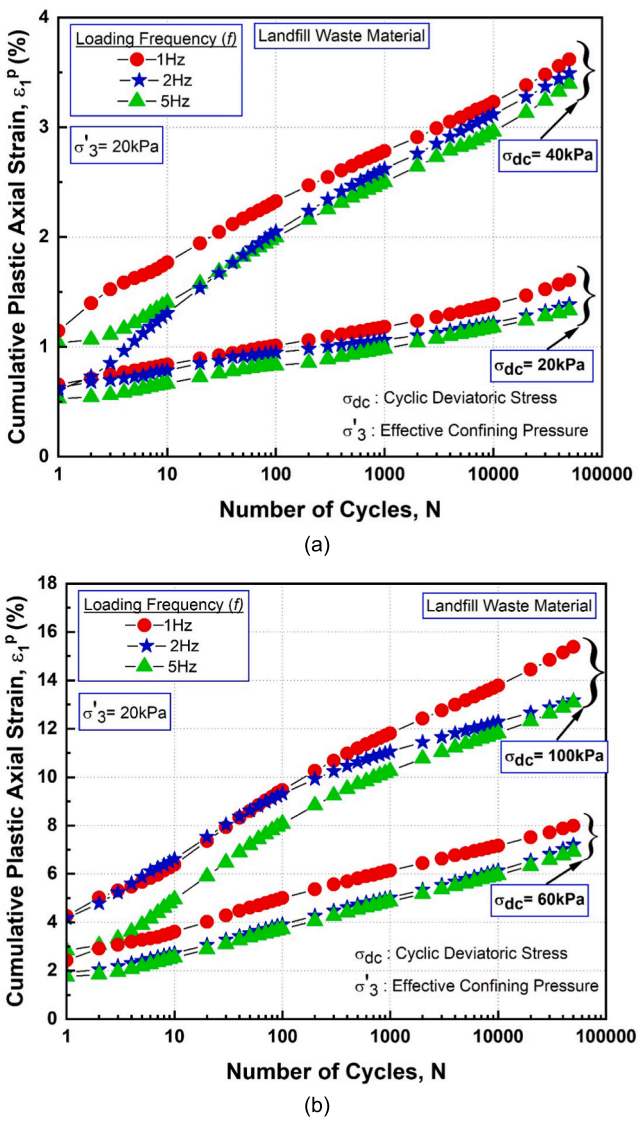

Fig. 9. Influence of loading frequency on cumulative plastic axial strain (ε_1^p) (a)(σ_{dc}) = 20 kPa and 40 kPa, (b)(σ_{dc}) = 60 kPa and 100 kPa.

Algorithm iteratively updates estimated parameters α, β and γ, as defined in Equation (1a), by approximating the model function within a dynamically adjusted region. This involves solving a quadratic model and adjusting the region size based on residual reduction until convergence criteria are met, making it effective for complex nonlinear models [57].Fig. 12 depicts the predicted plastic axial strains from Equation (1) compared with the data obtained from laboratory investigations within the 3D space. It is apparent from Fig. 12 that the proposed empirical equation demonstrates acceptable predictions, as supported by the coefficient of regression (R^2) value of 0.9581. Furthermore, the empirical model for cumulative plastic strain has been validated against the laboratory data from tests with cyclic deviatoric stress 40 kPa and 60 kPa with loading frequencies 1 Hz and 2 Hz, respectively, as presented in Fig. 13 (it should be noted that these data were not used to calibrate the model in Equation (1), thus could be readily used for validation purposes). It is evident that the values computed from the developed empirical Equation (1) align reasonably well with those obtained from the laboratory investigation, validating the accuracy of the proposed model.

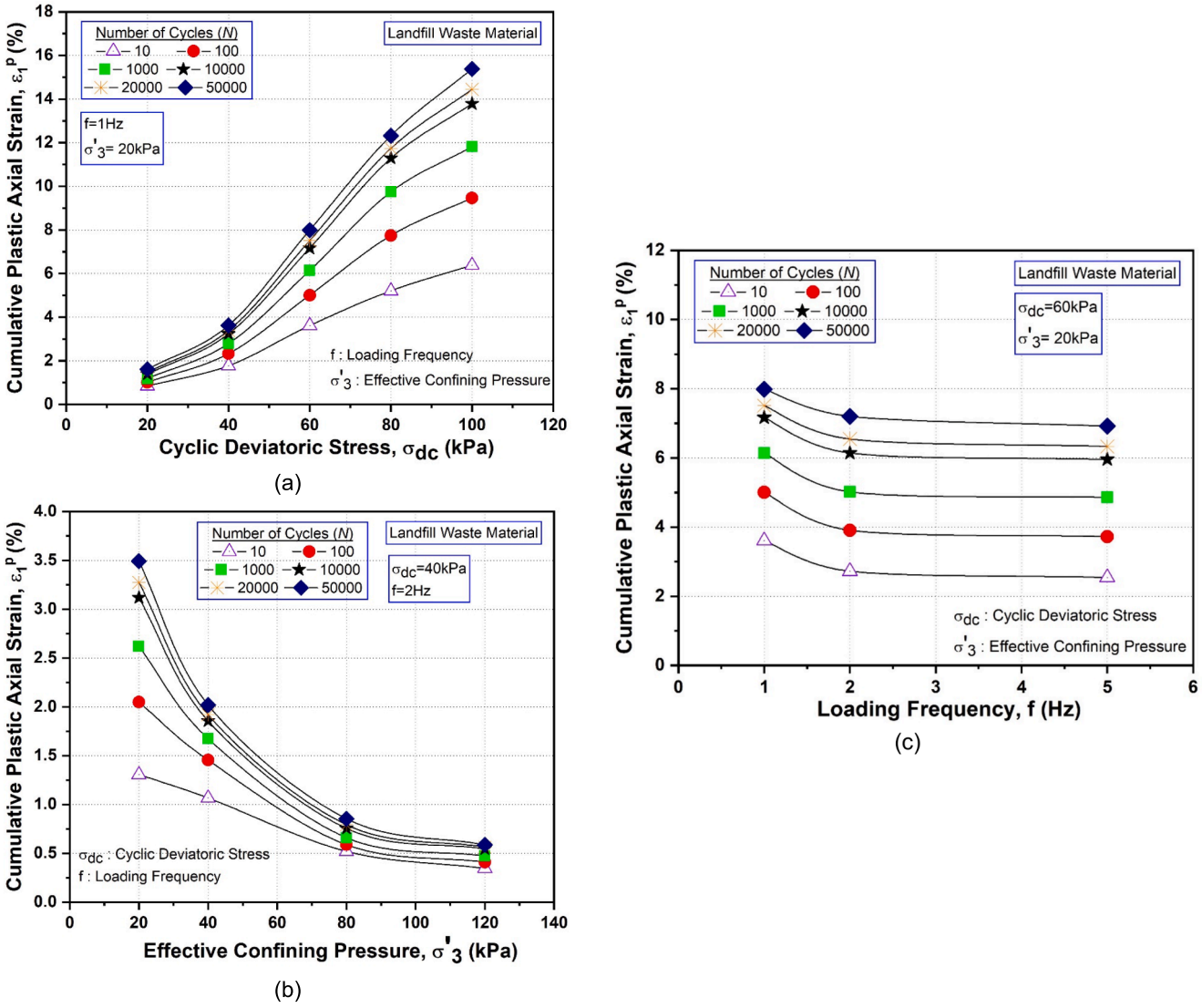

Fig. 10. Influence of (a) cyclic deviatoric stress (σ_{dc}), (b) effective confining stresses (σ'_3), and (c) loading frequency (f) on cumulative plastic axial strain (ε_1^p) at different cycles during cyclic loading.

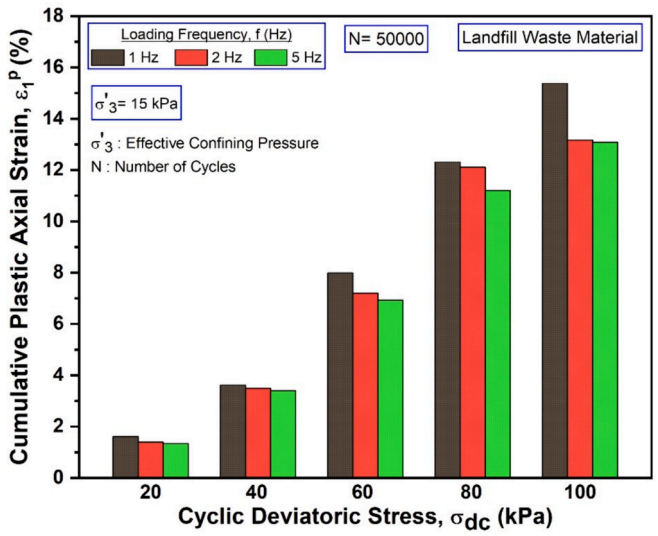

Fig. 11. Cumulative plastic axial strain (ε_1^p) observed at the end of the 50,000 cycles.

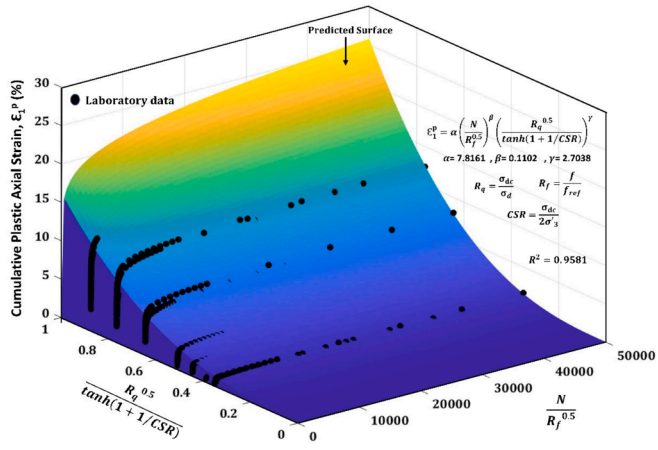

Fig. 12. Comparison of predicted cumulative plastic axial strain surface with laboratory data.

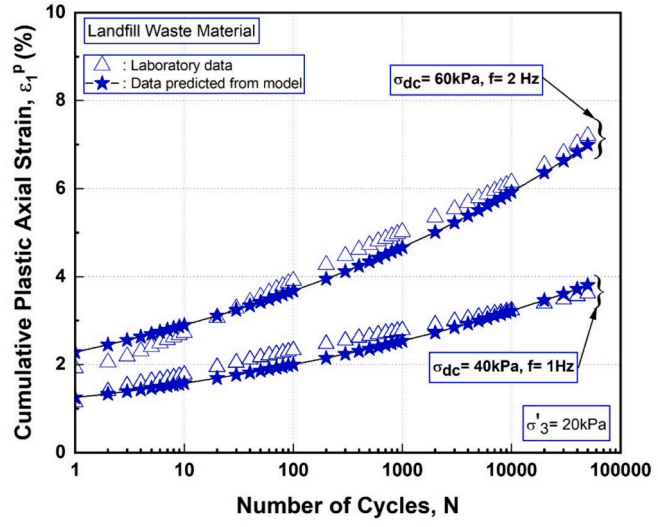

Fig. 13. Validation of the cumulative plastic axial strain predicted from the model with laboratory data.

3.4. Resilient modulus

The resilient modulus (M_R) is a parameter extensively utilised to elucidate the elastic deformation characteristics of a material exhibited during the unloading phase of cyclic loading and is defined as follows:

$$M_R = \frac{\sigma_{dc}}{\varepsilon_{1,rec}} \tag{2}$$

where σ_{dc} denotes the cyclic deviatoric stress also termed as cyclic stress amplitude, which is calculated as the difference between maximum and minimum cyclic deviatoric stresses, i.e. from the initial loading point to the subsequent unloading point, and $\varepsilon_{1,rec}$ represents elastic axial strain, recovered during unloading as schematically illustrated in Fig. 14. Figs. 15 - 17 illustrate the behaviour of resilient moduli of the reconstituted landfill waste specimens with loading cycles tested under different cyclic deviatoric stresses, confining pressures, and loading frequencies. Furthermore, the variation of resilient moduli corresponding to different cycle numbers with cyclic deviatoric stress, confining pressure, and loading frequency is depicted in Fig. 18. Fig. 19 presents the variation of resilient modulus at the last loading cycle with cyclic deviatoric stress and loading frequency. As the number of cycles increases, the resilient moduli of the reconstituted landfill waste specimens increase under all the tested conditions, as shown in Figs. 15 - 18. The resilient moduli exhibit a notable increase up to approximately 10,000 loading cycles, following which its rate gradually reduces. This behaviour is comparably more prominent under higher cyclic deviatoric stresses of 80 kPa and 100 kPa, whereas it is less pronounced under lower cyclic stress levels. Furthermore, referring to Figs. 15, 18a and 19, the resilient modulus increases with increasing deviatoric stress for a given confining pressure and loading frequency.

The observed resilient moduli response can be partly attributed to the rearrangement and reorientation of the waste components, resulting in the increased interlocking of the waste components over the course of multiple cycles. Interlocking of the waste components helps to distribute the applied load more effectively and simultaneously increases the mechanical properties of the landfill waste. Additionally, the fibrous material within the sample mobilises progressively as the strain increases and acts as reinforcement under tension, resulting in increased stiffness of the sample as the sample shears more. Indeed, the reinforcement effect of the fibrous material at higher strain values in static tests has been discussed by Zekkos [15]. Similar behaviour of M_R has been observed in the literature regarding the cyclic behaviour of fibre-reinforced soil, granular soil, and granular soil with the inclusion of rubber waste, as reported by Narani et al. [58], Bian et al. [59], and Qi et al. [60]. Correspondingly, with an increase in the confining pressure, the resilient moduli exhibit a significant escalation under the same cyclic deviatoric stress and loading frequency, as depicted in Figs. 16 and 18b. As discussed in the previous section, increasing confining stress leads to a significant reduction in the plastic deformation, as presented in Fig. 8, attributed to the bolstered waste-fibre matrix interaction resulting in the increased stiffness of the material, which in turn reduced the recoverable strain during the cyclic loading and consequently elevating the resilient modulus of the sample.

Furthermore, as the loading frequency increased, the resilient moduli demonstrated a slight increase for a given cyclic deviatoric stress and confining pressure, as illustrated in Figs. 17, 18c and 19. Moreover, referring to Fig. 18c and 19, it is apparent that the increase in the resilient moduli across different cycle numbers, as the frequency increases from 1 Hz to 2 Hz, is more pronounced than the increase observed from 2 Hz to 5 Hz. This observation is very much in line with the more pronounced decrease in cumulative plastic deformation in the lower frequency range from 1 Hz to 2 Hz, as discussed earlier and depicted in Fig. 9. Comparable trends have been observed by Keramati et al. [37] and Rawat et al. [61] in studies exploring the dynamic characteristics of municipal solid waste specimens subjected to cyclic

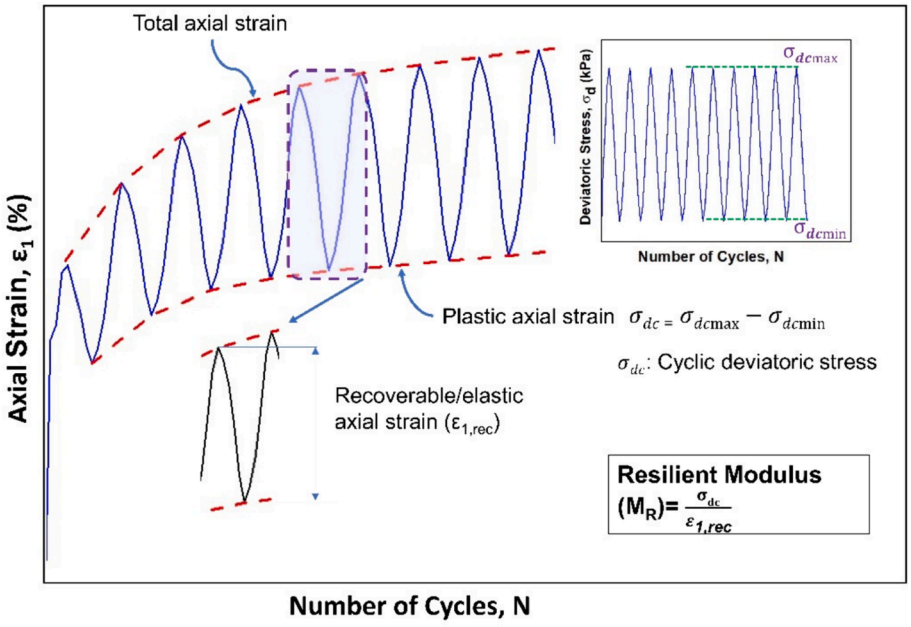

Fig. 14. Schematic illustration for resilient modulus calculation.

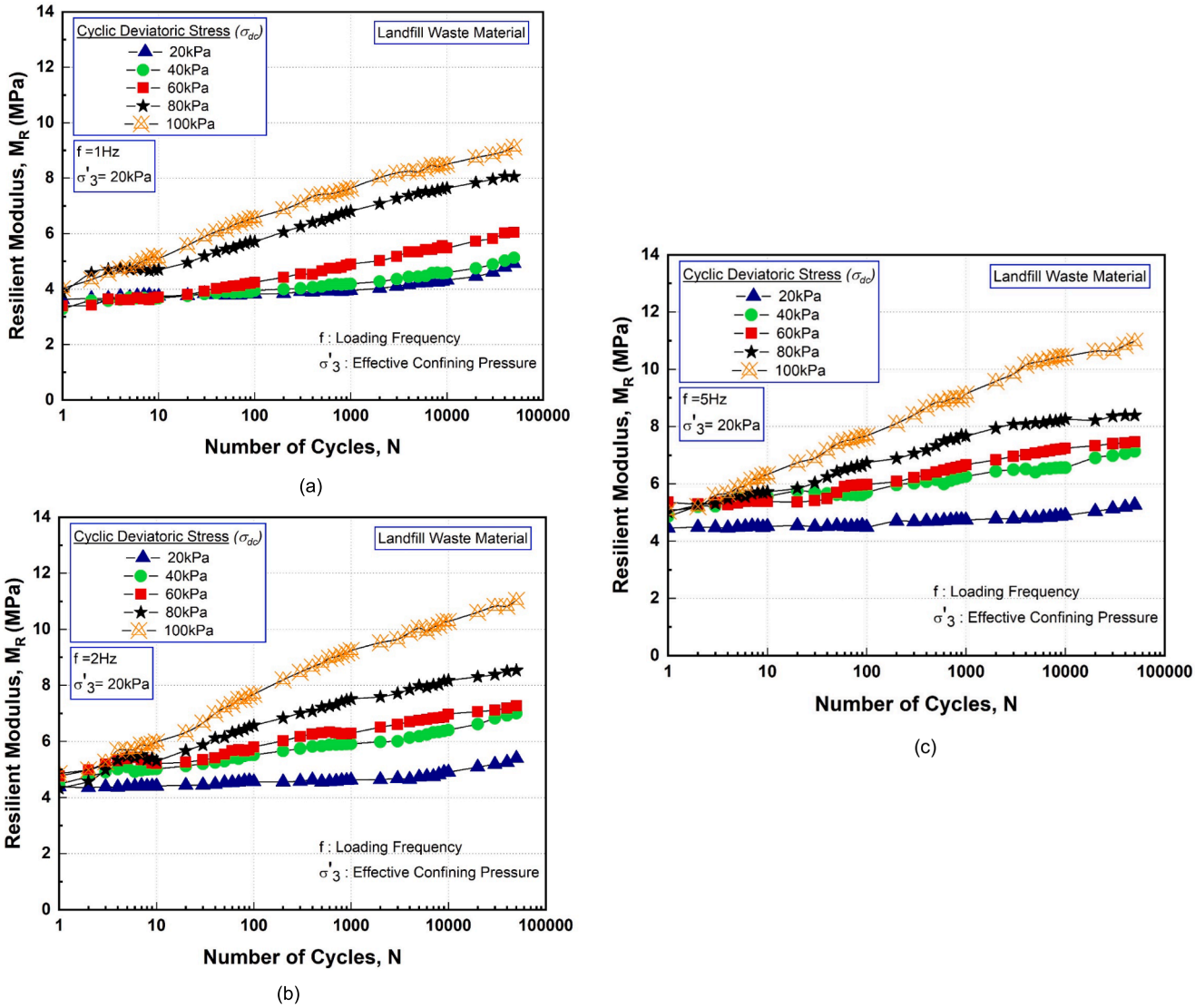

Fig. 15. Results of resilient modulus (M_R) vs number of cycles (N) under different cyclic deviatoric stresses (σ_{dc}) (a) $f = 1$ Hz, (b) $f = 2$ Hz, (c) $f = 5$ Hz.

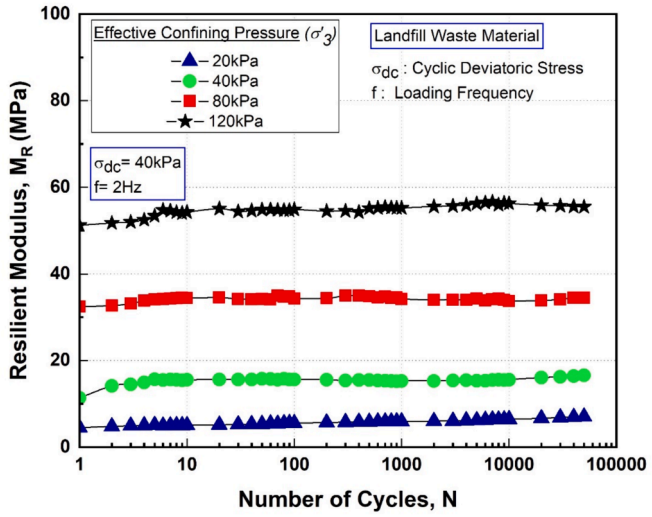

Fig. 16. Results of resilient modulus (M_R) vs number of cycles (N) under different effective confining stresses (σ'_3) under cyclic deviatoric stress (σ_{dc}) of 40 kPa.

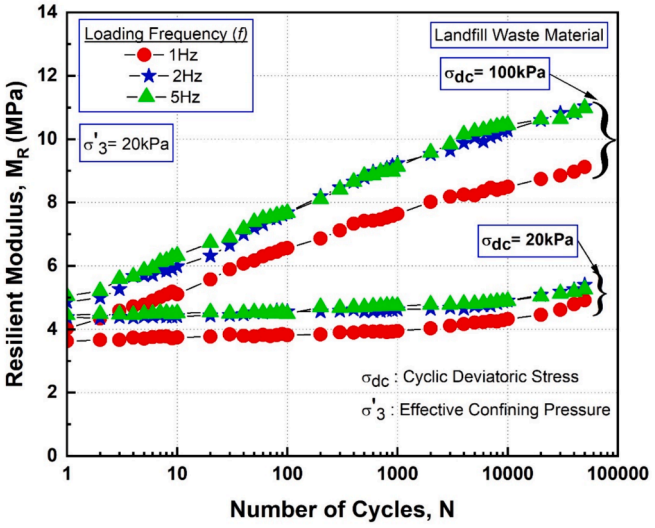

Fig. 17. Influence of loading frequency on resilient modulus (M_R), σ_{dc}= 20 kPa and 100 kPa.

loading. Zekkos [15] reported that the effect of the frequency on the stiffness of the landfill waste is rather negligible compared to the influence of the other parameters.

Based on the experimental results, variations of the resilient modulus with the cyclic deviatoric stress (σ_{dc}) are presented in Figs. 15 and 18a. Confirming this upward trend, an empirical relation was formulated between the normalised resilient modulus (R_M) (i.e. the ratio of the resilient modulus M_R to the undrained confined modulus E_{cu}), and the normalised cyclic deviatoric stress ratio (R_q), as presented in Fig. 20. This observed correlation serves as valuable information for practising engineers, enabling them to tentatively estimate the range of resilient modulus values of landfill waste materials based on the monotopic triaxial test results.

3.5. Damping ratio

The damping ratio (ξ) is a parameter extensively utilised to elucidate the damping characteristics of a material subjected to cyclic loading and is defined as the energy dissipation ratio that represents the proportion of energy that is dissipated compared to the maximum elastic energy stored during a loading–unloading cycle. As per ASTM-D3999 guidelines [62], the damping ratio for a particular hysteresis loop during cyclic loading can be determined as follows:

$$\xi = \frac{A_L}{\pi A_T} \tag{3}$$

where, A_L is the area enclosed by the hysteresis loop representing the energy dissipated by the specimen when subjected to a cyclic loading–unloading process and A_T is the area of the highlighted triangle representing the maximum elastic energy stored during the unloading, as schematically illustrated in Fig. 21. Figs. 22 - 24 present the variation of damping ratio per loading cycle values of the reconstituted landfill specimens with corresponding loading cycles tested under different cyclic deviatoric stresses, confining pressures, and loading frequencies. Furthermore, the variation of damping ratio per load cycle corresponding to different cycle numbers with cyclic deviatoric stress, confining pressure, and loading frequency is depicted in Fig. 25. As shown in Figs. 22 - 24, the damping ratio per load cycle values of the reconstituted landfill waste specimens decreases as the number of cycles increases for all the testing conditions. Comparable trends have been noted by Rawat et al. [61] in studies investigating the dynamic characteristics of municipal solid waste specimens and by Narani et al. [58] in the case of fibre-reinforced soil subjected to cyclic loading. Moreover, the rate of reduction of the damping ratio values was notably higher, up to approximately 10,000 loading cycles, following which the rate gradually reduced (refer to Figs. 22 - 24). The notable decline observed in the damping ratio of reconstituted waste specimens during the initial loading cycles can be elucidated by the observed increment in the plastic axial strain accumulation, as observed in Figs. 7 and 8. This behaviour could be primarily due to the particle rearrangement/reorientation, leading to increased energy dissipation alongside reduced energy storage. Nonetheless, as the plastic axial strain accumulation decelerates due to the increased interlocking between the waste components and the reinforcement effect due to the tension mobilisation of the fibres, the rate of energy dissipation correspondingly reduces, leading to the deceleration of the rate of damping ratio reduction as observed in Figs. 22 and 23.

Furthermore, referring to Figs. 22 and 25a, it is apparent that with an increase in the cyclic deviatoric stress, the damping ratio values increase. This behaviour can be attributed to the increased plastic axial strain occurring due to the application of elevated cyclic stresses, thereby increasing the dissipation of energy and leading to a subsequent increase in the damping ratio. Conversely, with an increase in the confining pressure, the damping ratio values exhibit a reduction, as depicted in Figs. 23 and 25b. The possible explanation for this response is that higher confining stresses facilitate a denser arrangement with enhanced bonding between the waste particles, thereby limiting their ability to deform, which is illustrated by the reduction in the cumulative plastic deformation presented in Fig. 8. Consequently, this reduces the dissipation of energy and, subsequently, lowers the damping ratios. Comparable trends for the damping ratio have been observed by Yuan et al. [34], and Zekkos et al. [35], where the damping ratio decreased at larger strains as the fibrous waste content increased and when tested under higher confining stresses. This effect is also partially attributed to

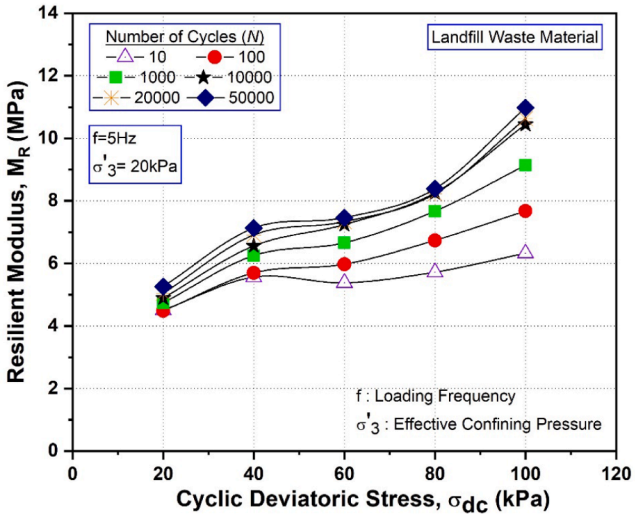

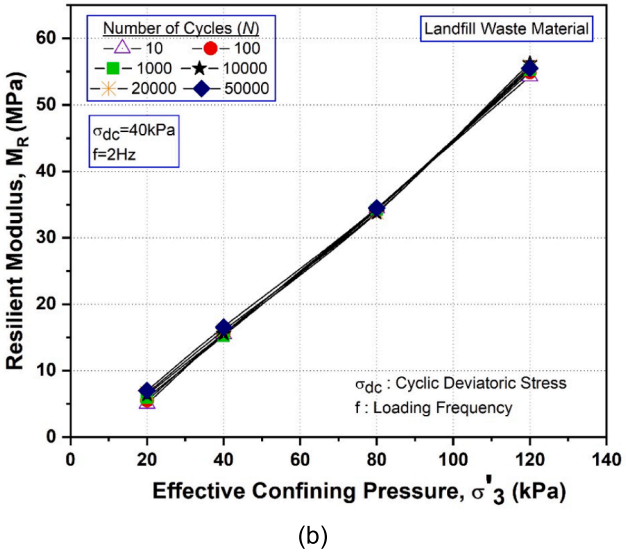

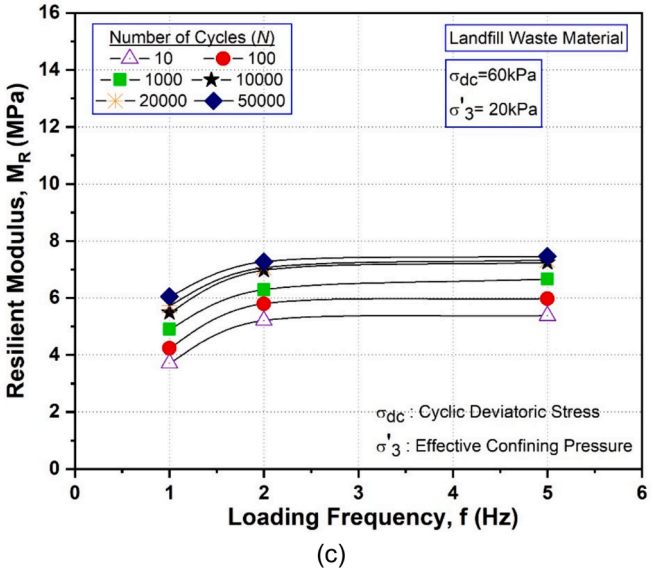

Fig. 18. Influence of (a) cyclic deviatoric stress (σ_{dc}), (b) effective confining stresses (σ_3'), and loading frequency (f) on resilient modulus (M_R) at different cycles during cyclic loading.

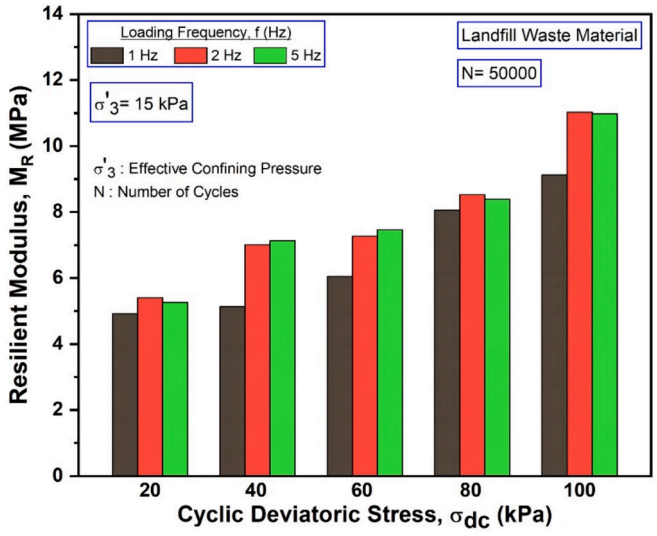

Fig. 19. Resilient modulus (M_R) observed at the end of the 50,000 cycles.

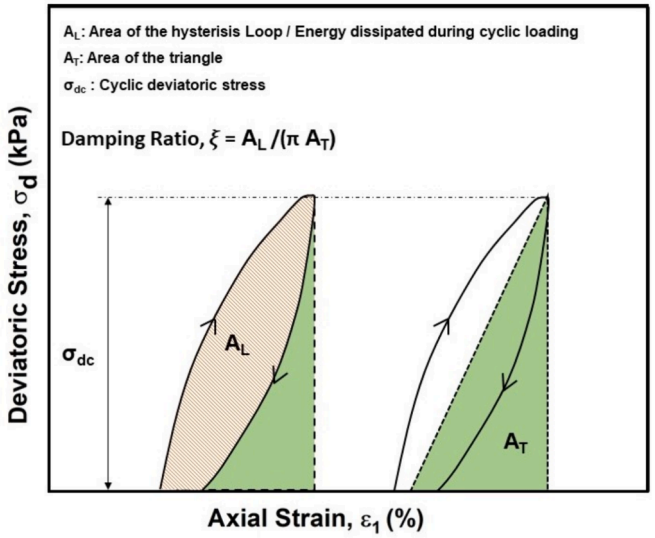

Fig. 21. Schematic illustration for damping ratio (ξ) calculation.

the orientation of the particles. In general, increasing the amounts of organic materials, rubber, and wood chips can amplify the damping and energy absorption of landfill waste. Furthermore, the damping ratio of the compacted landfill waste is insignificantly influenced by the loading frequency, as illustrated in Figs. 24 and 25c, which is in line with observed variations of the plastic strain reported in Figs. 9 and 10c.

3.6. Residual excess pore water pressure

When soil is subjected to cyclic loading, such as from traffic or train loads, pore water undergoes pressure changes. During the loading phase, the pore water pressure increases as the total stress increases and the soil tends to compress, and upon unloading, as the total stress decreases and soil tends to rebound, and thus, part of the excess pore water pressure

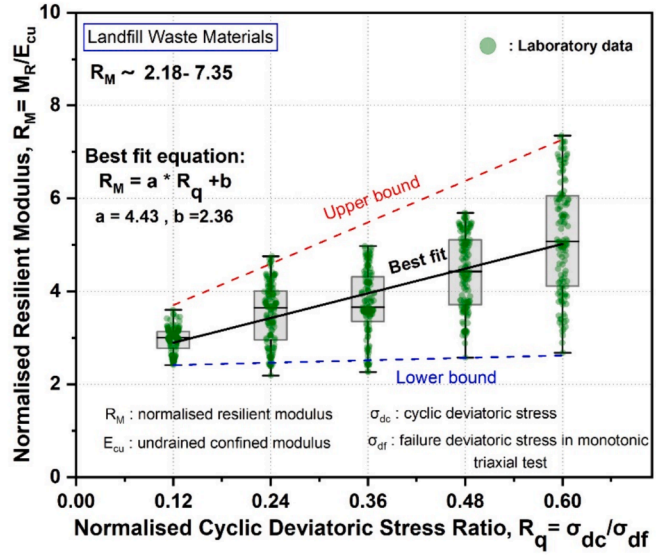

Fig. 20. Relationship established normalised resilient modulus (M_O) and the normalised cyclic deviatoric stress ratio (R_q).

would remain. This remaining pore water pressure at the end of unloading is known as residual excess pore water pressure (Δu_{ex}). Fig. 26 presents the Δu_{ex} of the reconstituted landfill waste specimens under different cyclic deviatoric stresses and loading frequencies. It is evident that the Δu_{ex} rises rapidly within the first few cycles, with a decreasing rate as the cyclic loading progresses. After 10,000 cycles, the residual excess pore water pressure Δu_{ex} stabilised in most cases, with a slight decrease observed in some of the tested samples. In addition, as indicated in Fig. 26, it is evident that as the cyclic deviatoric stress increases, the Δu_{ex} value also rises simultaneously under identical confining pressure and loading frequency conditions. The observed increase in the excess pore water pressure in this undrained cyclic triaxial loading can be attributed to the contractive response of the landfill sample. As the loading cycle progresses, the excess pore water pressure stabilises after a certain number of cycles, indicating that the sample is attaining the dynamic equilibrium where the rearrangement and orientation of the particles reaches to the state with no contraction or dilation tendency of the sample. This notion is further reinforced by the response of plastic deformation observed in Fig. 7. During the initial loading cycles, the rate of plastic deformation was notable, but as the loading cycle progressed, the rate of plastic deformation accumulation per loading cycle decreased significantly as evident in Fig. 7. Similar trends in excess pore water pressure have been observed by others while conducting dynamic testing on waste used as embankment material and peaty soil used as the foundation for railways [54,61].

4. Conclusions

This study experimentally assessed the dynamic characteristics of landfill waste, replicating conditions similar to a railway subgrade. The investigated parameters included cumulative plastic deformation, resilient modulus, and damping ratio, all of which were investigated using a cyclic triaxial setup. Drawing from experimental observations and analysis of results, several conclusions can be drawn regarding compacted landfill waste, which are summarized below.

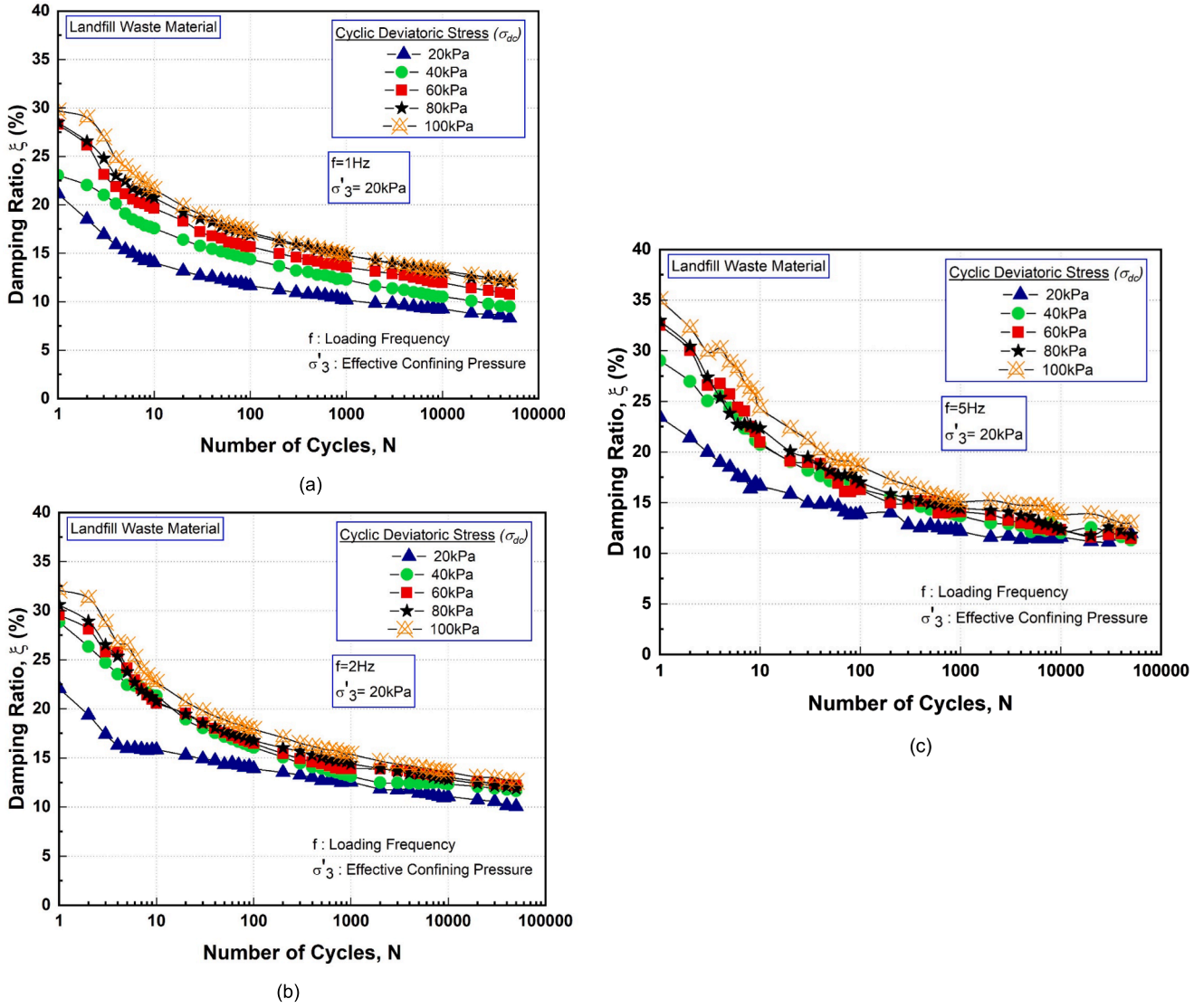

Fig. 22. Results of damping ratio (ξ) vs number of cycles (N) under different cyclic deviatoric stresses (σ_{dc}) (a) $f = 1$ Hz, (b) $f = 2$ Hz, (c) $f = 5$ Hz.

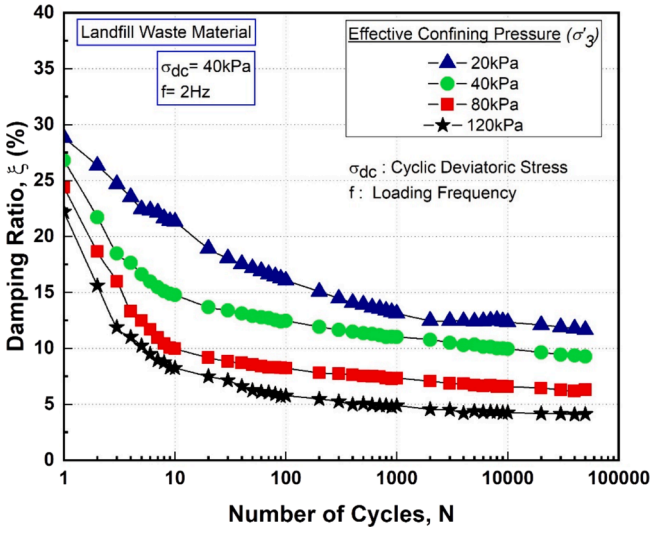

Fig. 23. Results of damping ratio (ξ) vs number of cycles (N) under different effective confining stresses (σ'_3) under cyclic deviatoric stress (σ_{dc}) of 40 kPa.

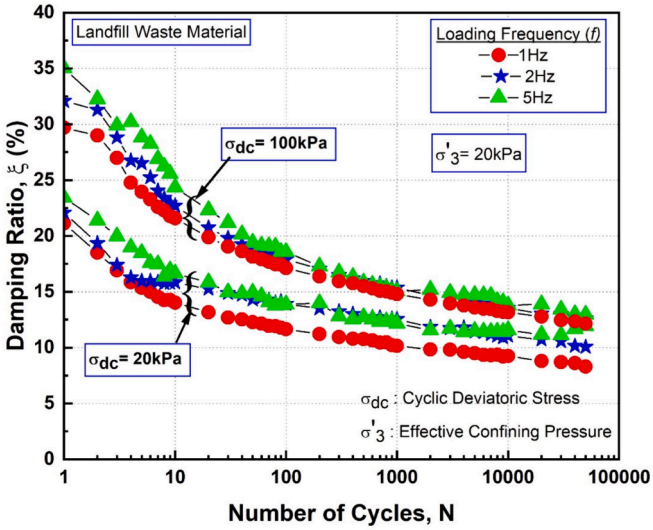

Fig. 24. Influence of loading frequency on damping ratio (ξ), σ_{dc}= 20 kPa and 100 kPa.

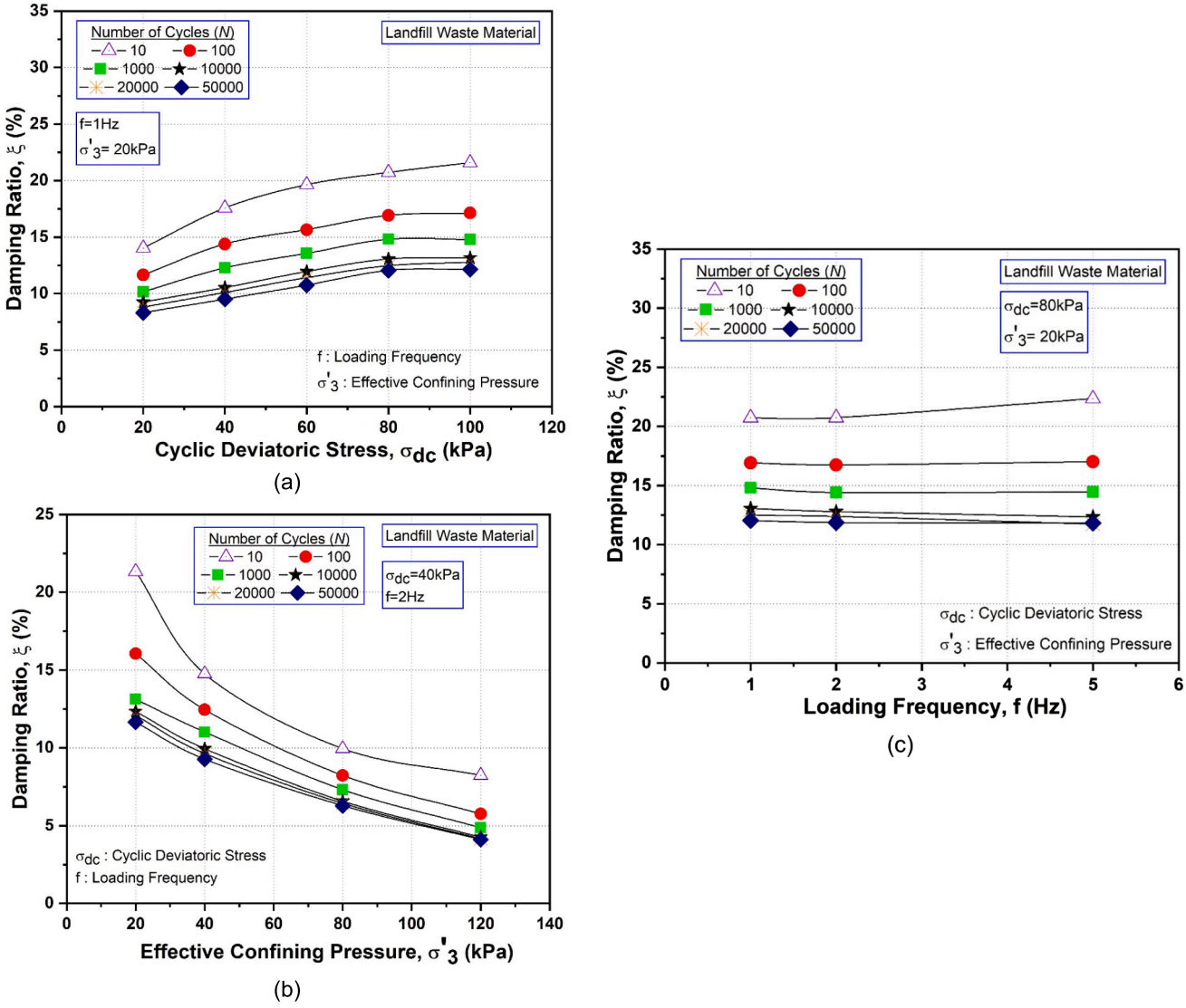

Fig. 25. Influence of (a) cyclic deviatoric stress (σ_{dc}), (b) effective confining stresses (σ'_3), and loading frequency (f) on damping ratio (ξ) at different cycles during cyclic loading.

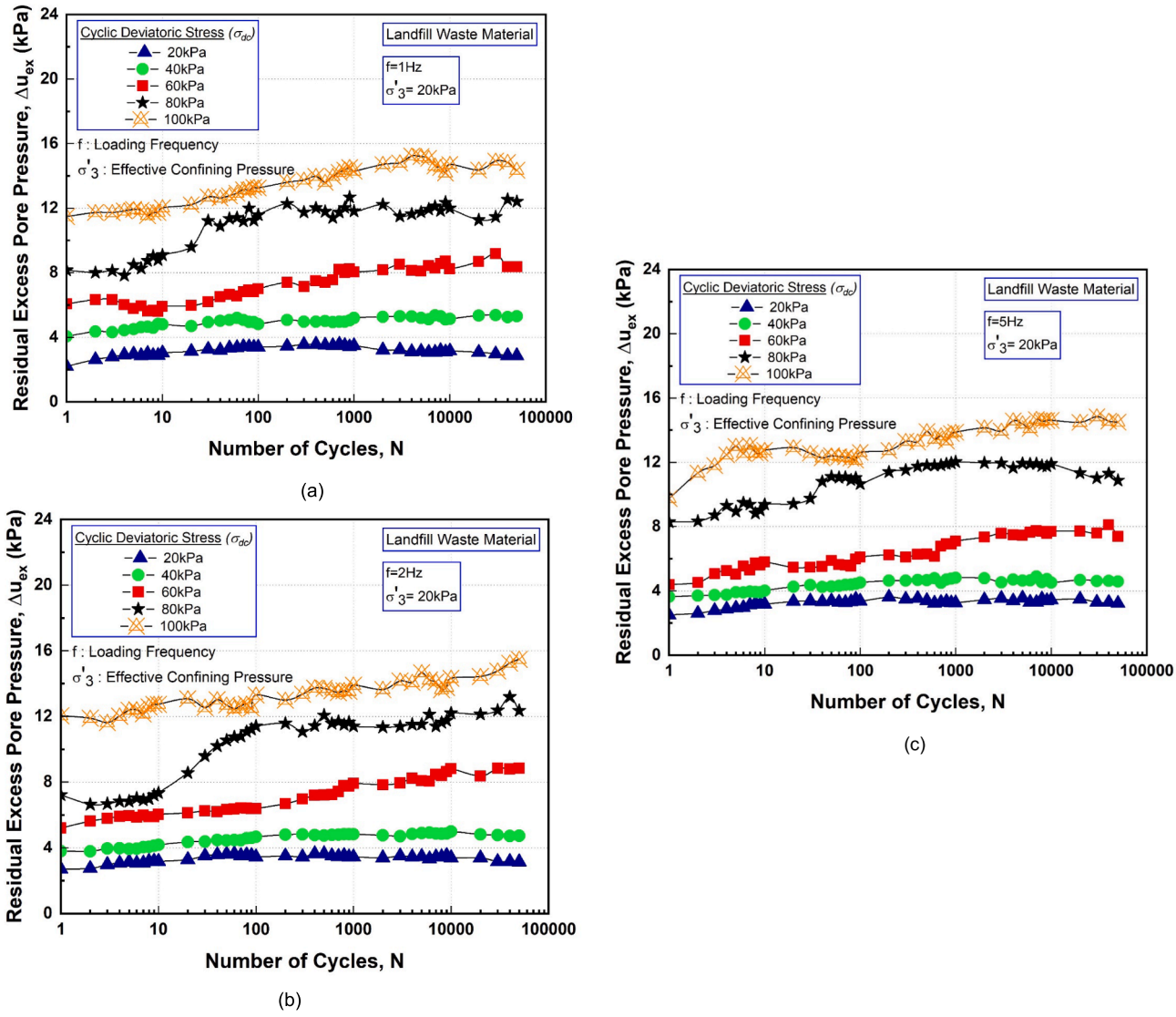

Fig. 26. Response of residual excess pore water pressure (Δu_{ex}) vs number of cycles (N) under different cyclic deviatoric stresses (σ_{dc}) (a) $f = 1$ Hz, (b) $f = 2$ Hz, (c) $f = 5$ Hz.

- The cumulative plastic axial strain (ε_1^p) consistently increased across all tested conditions throughout the loading cycles. As the cyclic deviatoric stress increased, the strain escalated for a given confining pressure and loading frequency. Moreover, the increase in confining stress showed a discernible decrease in plastic strain accumulation. However, the loading frequency imposed an insignificant impact compared to other investigated parameters.
- The cumulative plastic axial strain (ε_1^p) exhibited a rapid increase during the initial phase of the loading cycle. However, after approximately 10,000 cycles, the rate of increase in plastic strain notably decreased, indicating the attainment of a relatively stable state by the sample. A similar response has been observed in the case of residual excess pore water pressure, which increased significantly during the initial few loading cycles before reaching a stable condition. Additionally, this observed behaviour is also reflected in the stress–strain hysteresis loops, which initially appeared sparse but gradually became denser as the loading cycle progressed. A nonlinear regression analysis was conducted employing the nonlinear least square method along with the trust region algorithm to develop an empirical relation for cumulative plastic axial strain (ε_1^p) incorporating key parameters, including cyclic deviatoric stress, confining stress, number of cycles and frequency. This empirical relationship reported in Equation (1) enables design engineers to estimate the cumulative plastic deformation, resulting on permanent settlement of railway tracks built over the closed landfill sites.
- As the loading cycles progressed, the resilient modulus (M_R) of the reconstituted landfill waste specimens exhibited a noticeable increase across all tested conditions. This increase was particularly dominant during the initial 10,000 cycles, after which it either increased at a very small rate or remained almost constant. Moreover, the resilient modulus demonstrated a significant rise with confining pressure. However, its increment was comparatively minor with frequency compared to cyclic deviatoric stress and confining stress.
- The damping ratio (ξ) per load cycle of the reconstituted landfill waste specimens decreased as the number of cycles increased across all tested samples. Notably, there was a high rate of reduction in the damping ratio values up to approximately 10,000 loading cycles, after which this rate gradually diminished. Additionally, an increase in the cyclic deviatoric stress led to a subsequent increase in the damping ratio values. Conversely, for a given cyclic deviatoric stress and loading frequency, an increase in the confining pressure reduced the damping ratio. Interestingly, the loading frequency had a rather

insignificant influence on the damping ratio of the compacted landfill waste.

- The dynamic behaviour of landfill materials is significantly influenced by the rearrangement and reorientation of waste components occurring during the initial shear loading cycles. This rearrangement enhances the interlocking between waste components, consequently increasing the stiffness of the sample and aiding in resisting further deformation under similar loading conditions. Moreover, as the loading cycle progresses, fibre mobilisation occurs at higher strain levels, and the mobilised tensioned fibres serve as reinforcement, providing mechanical stiffening to the sample, similar to the behaviour observed in fibre-reinforced soils.

Overall, this research provides valuable insights into dynamic parameters essential for designing transport infrastructure, particularly when railway alignments intersect closed landfill sites, offering an opportunity to utilise the compacted landfill material as a railway track subgrade. By delving into the behaviour of landfill waste, the findings of this study contribute to a deeper understanding of how such landfill waste materials respond to dynamic loading conditions induced by moving trains. The findings empower design engineers and authorities with the essential knowledge required to predict the deformation of railway subgrade and deciding on any improvements and mitigation strategies required in case of excessive deformations and unsatisfactory performance.

CRediT authorship contribution statement

Sangharsha Bhandari: Writing – original draft, Visualization, Validation, Software, Methodology, Investigation, Conceptualization. **Behzad Fatahi:** Writing – review & editing, Visualization, Validation, Supervision, Project administration, Methodology, Investigation, Formal analysis, Conceptualization. **Waranga Habaraduwa Peellage:** Writing – review & editing, Validation, Software, Formal analysis. **Hadi Khabbaz:** Writing – review & editing, Supervision, Methodology, Investigation. **Haleh Rasekh:** Writing – review & editing, Supervision, Methodology, Investigation. **Jeff Hsi:** Writing – review & editing, Methodology, Investigation, Conceptualization.

Declaration of competing interest

The authors declare that they have no known competing financial interests or personal relationships that could have appeared to influence the work reported in this paper.

Data availability

Data will be made available on request.

Acknowledgements

The authors gratefully acknowledge the financial support and assistance provided by EIC Activities, CPB Contractors and CIMIC Group for facilitating site access and providing resources that enabled collecting the landfill samples. The laboratory testing was conducted using the facilities at the University of Technology Sydney (UTS). The authors sincerely thank Idy Li, Mr Hossein Haddad and Dr. Michael Vinod, who generously assisted with sample collection and shared their experience.

References

[1] AusGov, Waste Management Facilities in Australia. 2017, Geoscience Australia: https://data.aurin.org.au/.
[2] Bonaparte R, Bachus RC, Gross BA. geotechnical stability of waste fills: Lessons learned and continuing challenges. J Geotech Geoenviron Eng 2020;146(11): 05020010. https://doi.org/10.1061/(ASCE)GT.1943-5606.0002291.
[3] Emberton J, Parker A. The problems associated with building on landfill sites. Waste Management & Research: The Journal for a Sustainable Circular Economy 1987;5(1):473–82. https://doi.org/10.1177/0734242X8700500161.
[4] Mor S, Ravindra K. Municipal solid waste landfills in lower- and middle-income countries: Environmental impacts, challenges and sustainable management practices. Process Saf Environ Prot 2023;174:510–30. https://doi.org/10.1016/j.psep.2023.04.014.
[5] Zhang CI, et al. Physical, chemical, and engineering properties of landfill stabilized waste. Land Degrad Dev 2017;28(3):1113–21. https://doi.org/10.1002/ldr.2594.
[6] Korzeniowski W, Poborska-Młynarska K, Skrzypkowski K. The idea of the recovery of municipal solid waste incineration (MSWI) residues in Kłodawa Salt Mine SA by filling the excavations with self-solidifying mixtures. Arch Min Sci 2018;63(3).
[7] Bray JD, Zekkos D, Merry Scott M. Shear strength of municipal solid waste. J Geotech Geoenviron Eng 2017. https://doi.org/10.1061/41146(395)2.
[8] Dixon N, Jones DRV. Engineering properties of municipal solid waste. Geotext Geomembr 2005;23(3):205–33. https://doi.org/10.1016/j.geotexmem.2004.11.002.
[9] Gabr M, Valero S. Geotechnical properties of municipal solid waste. Geotech Test J 1995;18(2):241–51. https://doi.org/10.1520/GTJ10324J.
[10] Kavazanjian E, et al. Evaluation of MSW properties for seismic analysis. *Proceedings of the Specialty Conference on Geotechnical Practice in Waste Disposal. Part 1 (of 2)*. ASCE; 1995.
[11] Pelkey SA, Valsangkar AJ, Landva A. Shear displacement dependent strength of municipal solid waste and its major constituent. Geotech Test J 2001;24(4): 381–90. https://doi.org/10.1520/GTJ11135J.
[12] Powrie W, Beaven RP. Hydraulic properties of household waste and implications for landfills. Proceedings of the Institution of Civil Engineers - Geotechnical Engineering 1999;137(4):235–7. https://doi.org/10.1680/gt.1999.370409.
[13] Reddy KR, et al. Geotechnical properties of fresh municipal solid waste at Orchard Hills Landfill, USA. Waste Manag 2009;29(2):952–9. https://doi.org/10.1016/j.wasman.2008.05.011.
[14] Vilar OM, Carvalhod M. Mechanical properties of municipal solid waste. J Test Eval 2004;32(6). https://doi.org/10.1520/JTE11945.
[15] Zekkos, D., *Evaluation of static and dynamic properties of municipal solid -waste*, J.D. Bray, Editor. 2005, ProQuest Dissertations Publishing.
[16] Landva AO, Clark JI. Geotechnics of waste fill. Geotechnics of waste fills—Theory and practice. ASTM International; 1990.
[17] Santos SM, Jucá J, Aragao J. Geotechnical properties of a solid waste landfill: Muribeca's case. *Proc. of the Third International Congress on Environmental Geotechnics*.. 1998.
[18] Gomes C, et al. Sanitary landfill of Santo Tirso-municipal waste physical, chemical and mechanical properties. Proc., 4th Int. Congress on Environmental Geotechnics. 2002.
[19] Pereira A, Sopena L, Mateos T. *Compressibility of a municipal solid waste landfill*. Proc., 4th Int. Congress on Environmental Geotechnics. 2002.
[20] Haddad H, et al. Effects of stress history on compressibility characteristics of undisturbed landfill waste material. Constr Build Mater 2024;422:135725.
[21] Brown SF, Lashine AKF, Hyde AFL. Repeated load triaxial testing of a silty clay. Géotechnique 1975;25(1):95–114. https://doi.org/10.1680/geot.1975.25.1.95.
[22] Cai YQ, et al. Stress–strain response of soft clay to traffic loading. Géotechnique 2017;67(5):446–51. https://doi.org/10.1680/jgeot.15.P.224.
[23] Li D, Selig ET. Resilient modulus for fine-grained subgrade soils. J Geotech Eng 1994;120(6):939–57. https://doi.org/10.1061/(ASCE)0733-9410(1994)120:6(939).
[24] Li D, Selig ET. Cumulative plastic deformation for fine-grained subgrade soils. J Geotech Geoenviron Eng 1996;122(12):1006–13. https://doi.org/10.1061/(ASCE)0733-9410(1996)122:12(1006).
[25] Preteseille M, Lenoir T. Structural test at the laboratory scale for the utilization of stabilized fine-grained soils in the subgrades of High Speed Rail infrastructures: Experimental aspects. Int J Fatigue 2016;82:505–13. https://doi.org/10.1016/j.ijfatigue.2015.09.005.
[26] Guo L, et al. Undrained deformation behavior of saturated soft clay under long-term cyclic loading. Soil Dyn Earthq Eng 1984;2013(50):28–37. https://doi.org/10.1016/j.soildyn.2013.01.029.
[27] Jiang, M., et al., *Effect of Cyclic Loading Frequency on Dynamic Properties of Marine Clay*. 2010. p. 240-245.
[28] Liu J, Xiao J. Experimental study on the stability of railroad silt subgrade with increasing train speed. J Geotech Geoenviron Eng 2010;136(6):833–41. https://doi.org/10.1061/(ASCE)GT.1943-5606.0000282.
[29] Naeini M, et al. Stiffness and strength characteristics of demolition waste, glass and plastics in railway capping layers. Soils Found 2019;59(6):2238–53. https://doi.org/10.1016/j.sandf.2019.12.009.
[30] Noura S, et al. Fatigue and stiffness characteristics of asphalt mixtures made of recycled aggregates. Int J Fatigue 2023;174:107714. https://doi.org/10.1016/j.ijfatigue.2023.107714.
[31] Augello AJ, et al. Dynamic properties of solid waste based on back-analysis of oii landfill. J Geotech Geoenviron Eng 1998;124(3):211–22. https://doi.org/10.1061/(ASCE)1090-0241(1998)124:3(211).
[32] Lee JJ. Dynamic characteristics of municipal solid waste (MSW) in the linear and nonlinear strain ranges. ProQuest Dissertations Publishing; 2007.
[33] Sahadewa A, et al. In-situ assessment of the dynamic properties of municipal solid waste at a landfill in texas. Soil Dyn Earthq Eng 2014;65:303–13. https://doi.org/10.1016/j.soildyn.2014.04.004.
[34] Yuan P, et al. Compositional effects on the dynamic properties of municipal solid waste. Waste Manag 2011;31(12):2380–90. https://doi.org/10.1016/j.wasman.2011.07.009.

[35] Zekkos D, Bray JD, Riemer MF. Shear modulus and material damping of municipal solid waste based on large-scale cyclic triaxial testing. Can Geotech J 2008;45(1): 45–58. https://doi.org/10.1139/T07-069.
[36] Naveen B, Sitharam T, Sivapullaiah P. Evaluating the dynamic characteristics of municipal solid waste for geotechnical purpose. Curr Adv Civ Eng 2014;2(1): 28–34.
[37] Keramati M, et al. Effect of confining stress and loading frequency on dynamic behavior of municipal solid waste in Kahrizak landfill. Int J Environ Sci Technol 2018;15(6):1257–64. https://doi.org/10.1007/s13762-017-1465-1.
[38] Towhata I, Uno M. Cyclic shear tests of municipal waste in large triaxial device for identification of its dynamic properties. In: *Geotechnical earthquake engineering and soil dynamics IV*; 2008. p. 1–10.
[39] ASTM-D2216-19, *Standard test methods for laboratory determination of water (moisture) content of soil and rock by mass.* D2216-10). ASTM International, West Conshohocken, PA. doi, 2019. **10**.
[40] ASTM-D2974-20e1. *Standard test methods for determining the water (moisture) content, ash content, and organic material of peat and other organic soils*. 2020. ASTM West Conshohocken, PA.
[41] ASTM-D698, *Standard Test Methods for Laboratory Compaction Characteristics of Soil Using Standard Effort (12 400 ft-lbf/ft3 (600 kN-m/m3))*. 2012.
[42] Miller GA, et al. Cyclic shear strength of soft railroad subgrade. J Geotech Geoenviron Eng 2000;126(2):139–47. https://doi.org/10.1061/(ASCE)1090-0241(2000)126:2(139).
[43] Yang J-Q, Cui Z-D. Influences of train speed on permanent deformation of saturated soft soil under partial drainage conditions. Soil Dyn Earthq Eng 2020;133 (1984):106120. https://doi.org/10.1016/j.soildyn.2020.106120.
[44] Gräbe PJ, Clayton CR. Effects of principal stress rotation on permanent deformation in rail track foundations. J Geotech Geoenviron Eng 2009;135(4): 555–65. https://doi.org/10.1061/(ASCE)1090-0241(2009)135:4(555).
[45] Rhylane H, Ajdour M. Dynamic analysis of railway track response subjected to train moving loads using finite element simulation. Transportation Infrastructure Geotechnology 2023. https://doi.org/10.1007/s40515-023-00300-7.
[46] Mamou A, et al. Behaviour of saturated railway track foundation materials during undrained cyclic loading. Can Geotech J 2018;55(5):689–97. https://doi.org/10.1139/cgj-2017-0196@cgj-ec.2018.01.issue-7.
[47] Powrie W, Yang LA, Clayton CRI. *Stress changes in the ground below ballasted railway track during train passage*. Proceedings of the Institution of Mechanical Engineers. Part F, Journal of rail and rapid transit. 2007;221(2):247–62. https://doi.org/10.1243/0954409JRRT95.
[48] Selig ET, Waters JM. *Track geotechnology and substructure management*. London, England: Thomas Telford Services Ltd; 2007.
[49] Martínez-Casas J, et al. Numerical estimation of stresses in railway axles using a train–track interaction model. Int J Fatigue 2013;47:18–30. https://doi.org/10.1016/j.ijfatigue.2012.07.006.
[50] Narani SS, et al. Evaluation of fiber-reinforced and cement-stabilized rammed-earth composite under cyclic loading. Constr Build Mater 2021;296:123746. https://doi.org/10.1016/j.conbuildmat.2021.123746.
[51] Oliveira PJV, Anunciação GR, Correia AAS. Effect of cyclic loading frequency on the behavior of a stabilized sand reinforced with polypropylene and sisal fibers. J Mater Civ Eng 2022;34(1). https://doi.org/10.1061/(ASCE)MT.1943-5533.0004012.
[52] Oliveira, P.J.V., A.A.S. Correia, and J.C.A. Cajada, *Effect of the type of soil on the cyclic behaviour of chemically stabilised soils unreinforced and reinforced with polypropylene fibres.* Soil dynamics and earthquake engineering (1984), 2018. **115** (C): p. 336-343 Doi: 10.1016/j.soildyn.2018.09.005.
[53] Tang Y, et al. Resilient and plastic strain behavior of freezing-thawing mucky clay under subway loading in Shanghai. Nat Hazards 2014;72(2):771–87. https://doi.org/10.1007/s11069-014-1036-4.
[54] Chen C, et al. Behavior of amorphous peaty soil under long-term cyclic loading. Int J Geomech 2018;18(9):27–52. https://doi.org/10.1061/(ASCE)GM.1943-5622.0001254.
[55] Zhang B, Wang D, Lei L. Dynamic deformation characteristics of frozen clay under pure principal stress rotation. Arab J Geosci 2022;15(3). https://doi.org/10.1007/s12517-022-09572-8.
[56] Monismith CL, Ogawa N, Freeme C. Permanent deformation characteristics of subgrade soils due to repeated loading. Transp Res Rec 1975;537.
[57] Gould N, Orban D, Toint P. Numerical methods for large-scale nonlinear optimization. Acta Numerica 2005;14:299–361. https://doi.org/10.1017/S0962492904000248.
[58] Narani SS, et al. Long-term dynamic behavior of a sandy subgrade reinforced by Waste Tire Textile Fibers (WTTFs). Transp Geotech 2020;24:100375. https://doi.org/10.1016/j.trgeo.2020.100375.
[59] Bian X, et al. Cyclic and postcyclic triaxial testing of ballast and subballast. J Mater Civ Eng 2016;28(7). https://doi.org/10.1061/(ASCE)MT.1943-5533.0001523.
[60] Qi Y, et al. Effect of rubber crumbs on the cyclic behavior of steel furnace slag and coal wash mixtures. J Geotech Geoenviron Eng 2018;144(2). https://doi.org/10.1061/(ASCE)GT.1943-5606.0001827.
[61] Rawat P, Mohanty S. Parametric study on dynamic characterization of municipal solid waste fine fractions for geotechnical purpose. Journal of hazardous, toxic and radioactive waste 2022;26(1). https://doi.org/10.1061/(ASCE)HZ.2153-5515.0000659.
[62] ASTM-D3999, *D3999 Standard Test Methods for the Determination of the Modulus and Damping Properties of Soils Using the Cyclic Triaxial Apparatus*. 2011.